Interaction of energetic particles with surfaces: insight from molecular-dynamics simulations

H. M Urbassek

Physics Dept., University of Kaiserslautern, Germany

Thanks to: Chr. Anders, S. Zimmermann,
A. Friedrich, Y. Rosandi, C. Engin
E. Bringa (LLNL),
R. E. Johnson (U Virginia)

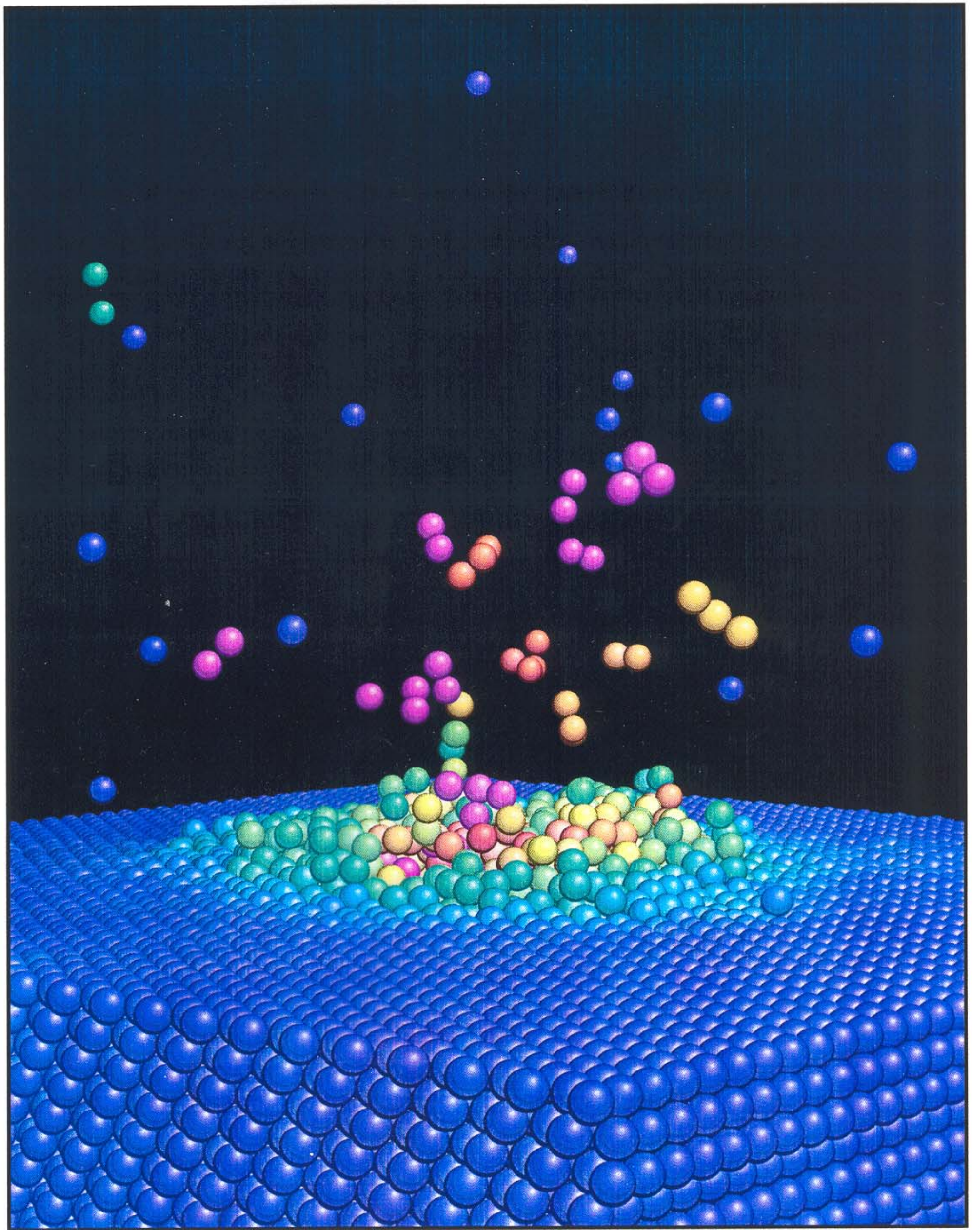

5 keV Cu $\rightarrow$ Cu
after 1 ps
color: temperature
(kinetic energy
in the center-of-mass
frame)

Particle-solid interaction: applications:

- materials production:
  - implantation
  - ion-beam mixing
- surface technology:
  - thin-film growth
  - etching
  - surface modification
- micro- and nano-fabrication
- surface analysis:
  - depth profiling
  - SIMS, RBS, ...
- biotechnology:
  - desorption of biomolecules
- plasma-wall interaction:
  - thermonuclear fusion
- astrophysics:
  - erosion of planets, comets, dust grains

Characteristics of molecular dynamics

Solve Newton‘s equations.

Think of:

Potentials: empirical many-body potentials
Electrons: no excitation or: friction-like energy loss
Boundary conditions: sufficiently large crystallite
Detectors: atomistic
Statistics: sufficiently many atoms

Advantages

- as realistic as possible in comparison to analytical theory or Monte Carlo simulations

  - for many-body simulations

  - for thermal nonequilibrium situations

- easy visualization / animation:

  appeals to imagination

Disadvantages

- slow
- cannot handle time scales $\gtrsim$ 1 ns
- cannot handle space scales $\gtrsim$ 100 nm

Metallic many-body potentials

(EAM potentials, tight-binding potentials, ...)
Describe for fcc metals reasonably:

- lattice constant, cohesive energy
- elastic constants
- defect energies
- extended defects, impurities
- surface structure

Outline:

- 'spikes' in metals induced by keV atom impact
- change in surface topography by ion bombardment
- cluster-induced cratering: linking nano- and microscales

High-density cascades: Spikes

Herbert M Urbassek

Physics Department
University of Kaiserslautern
Germany

A spike is a limited volume with the majority of atoms temporarily in motion.

Spike effects may be important when the spike lifetime is larger than the duration of the initiating cascade. Spikes have been considered as the origin of a variety of experimental results over the years. The more compelling evidence seems to come from sputtering experiments.

Peter Sigmund, Appl. Phys. Lett. 1974
Energy density and time constant of heavy-ion-induced elastic-collision spikes in solids

Spikes used to explain:

Sputtering:	enhancement,
	esp. under cluster bombardment
Damage:	reduction of point defect production
	defect structure *(cascade collapse)*
	amorphization
	surface topography *(craters)*
	chemical disorder *(ordered alloys)*
Mixing:	enhancement
	in molten cascade core
Conceptual:	use of macroscopic concepts
	n, T, p

<u>n, T, p:</u>

System:

- 1 keV Cu $\rightarrow$ Cu
- many-body potential
- no electronic stopping
- $\cong 10^4$ atoms
- 5 ps simulated

Data analysis:

- macroscopic quantities as *gliding averages* over sphere with radius $r_c = 4.7$ Å containing $\cong 43$ atoms
- temperature from

- only potential contribution to pressure from virial

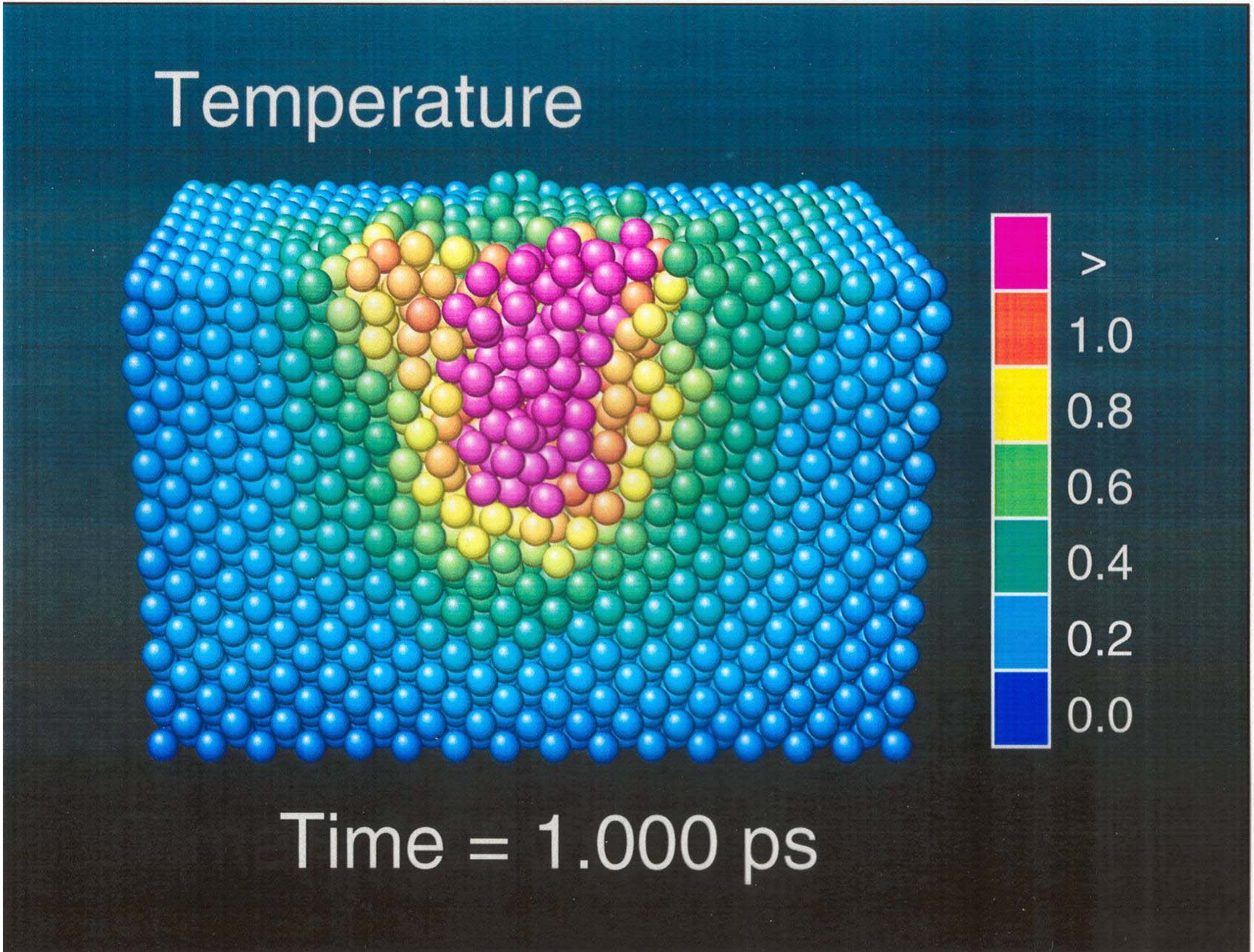
Temperature
>
1.0
0.8
0.6
0.4
0.2
0.0
Time = 1.000 ps

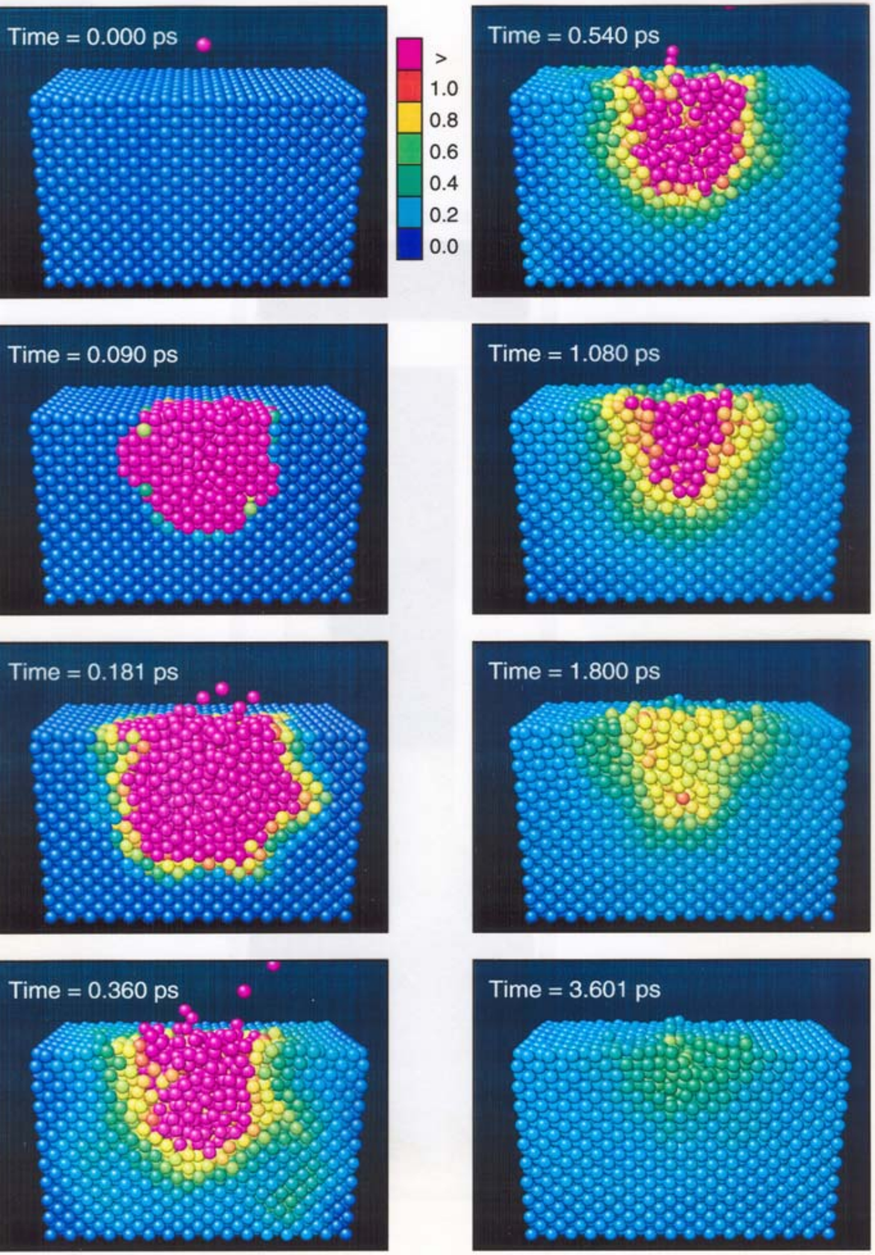

Th. J. Colla and H. M. Urbassek [cf. Radiat. Eff. 142, 439-447 (1997)]:
Cross section through a Cu(100) crystal after bombardment with a 1keV Cu ion.
Kinetic energy ("temperature") in units of $\frac{3}{2}kT_{melt}$ shown as gliding average around each atom.

movie:
[1 keV Cu -> Cu]

E_{pot}, E_{kin}
in molten region

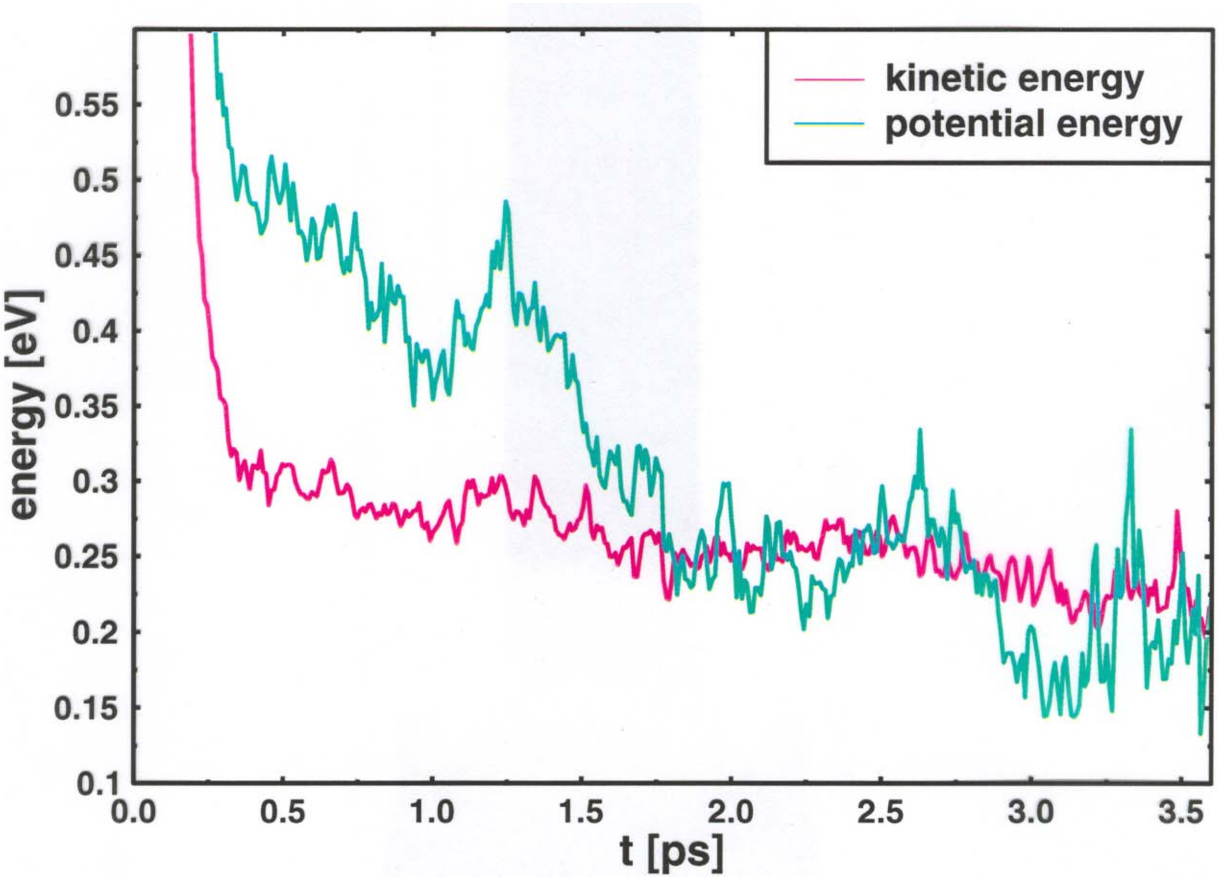

$E_{pot} - E_{kin}$: $L_{melt} = 0.14$ eV /atom

latent heat of melting

Cascade melting

Check:

- latent heat
- temperature
- diffusion
- pair correlation

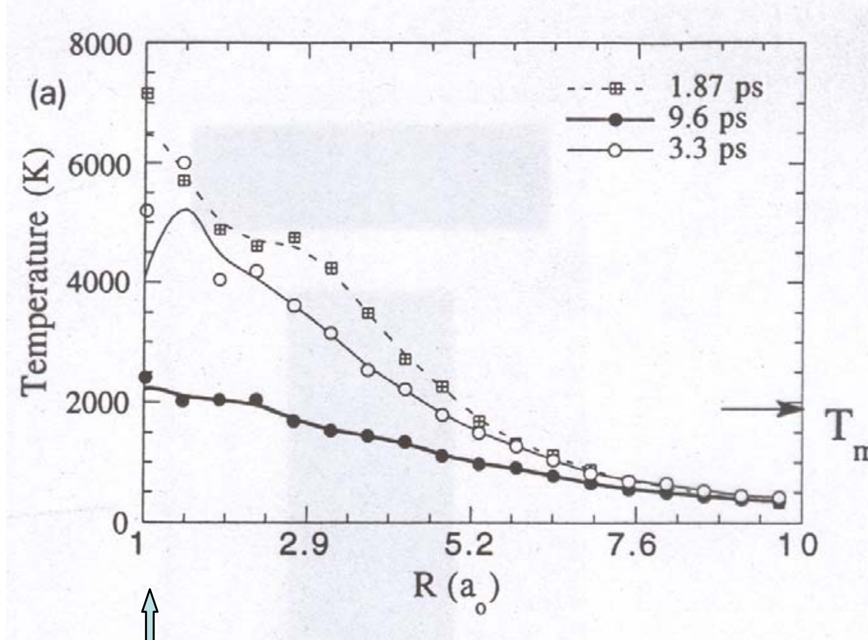

10 keV Au -> Au
temperature vs
distance from spike center
Averback & Ghaly, 1994

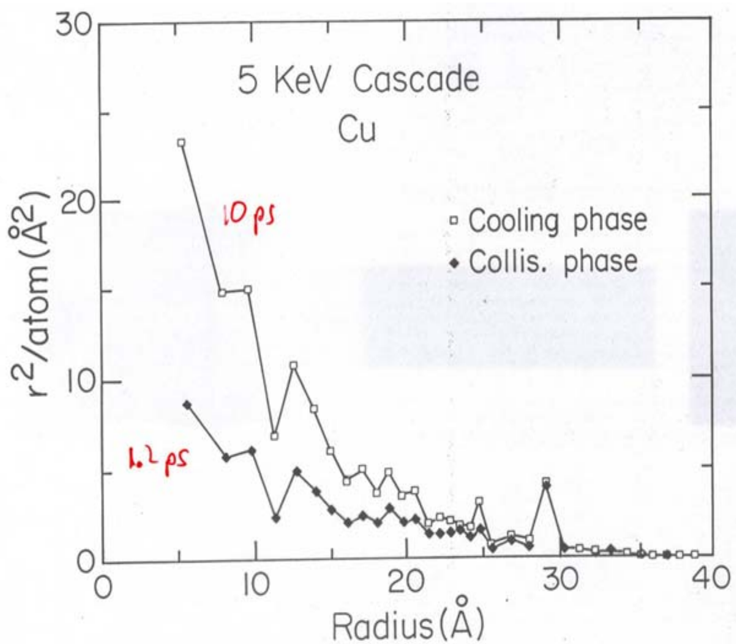

mean square diplacement
Averback et al 1988

Fig. 8

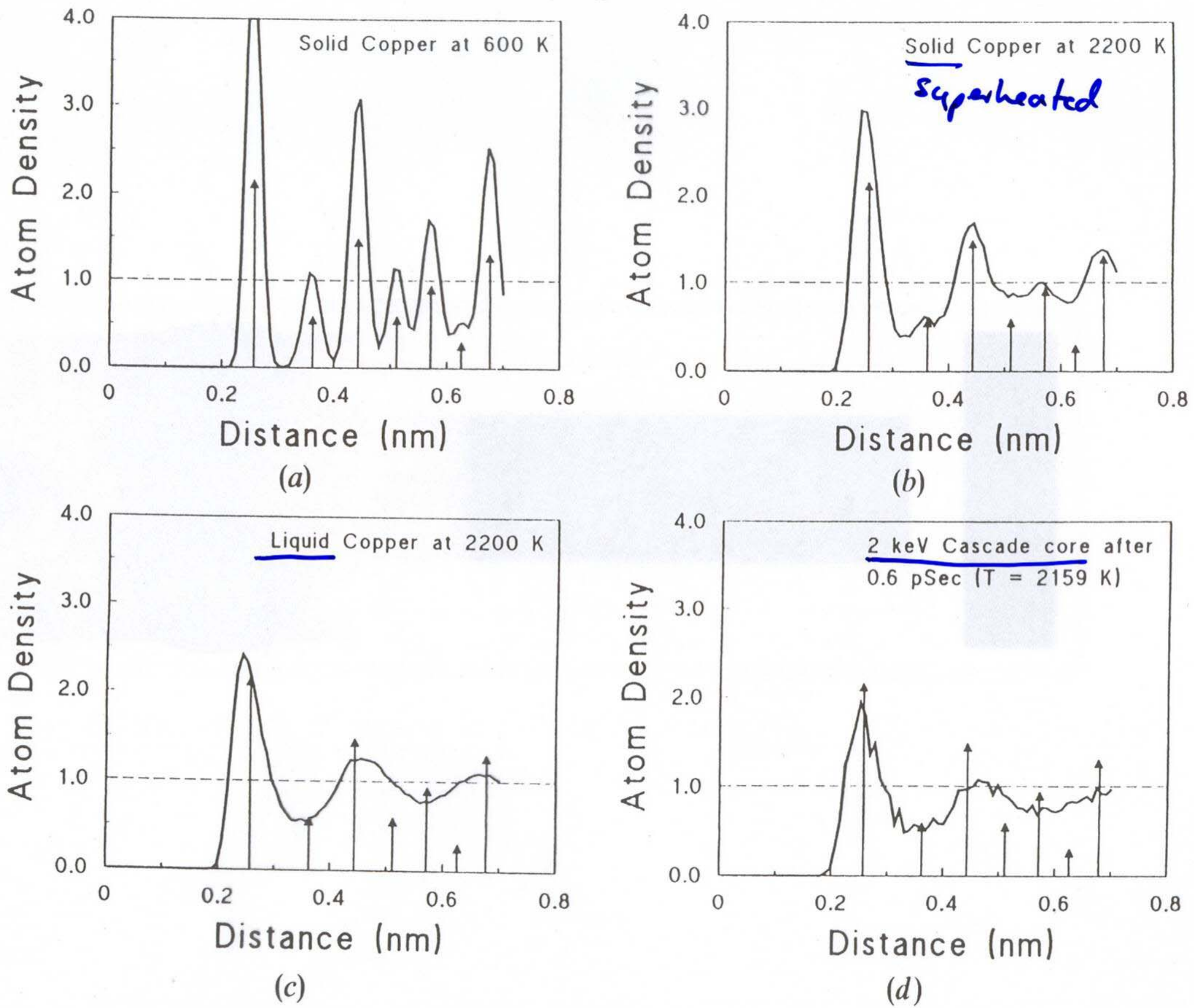

Radial distribution functions for copper at (*a*) 600 K, (*b*) superheated to 2200 K and (*c*) liquid at 2200 K. Compare with (*d*) the core of a 2 keV cascade after 0·6 ps.

Foreman

Cascade melting: Conclusions:

- liquid at low density
- low lattice heat capacity $\rightarrow$ long spike lifetime
- importance of latent heat of melting $\rightarrow$ long spike lifetime
- Pressure relaxation at free surface

Changes in surface topography due to single ion impact

H. Gades, C. Engin, A. Friderich, Y. Rosandi,
H. M Urbassek

Physics Dept., University of Kaiserslautern, Germany

Thanks to: Th. Michely, H. Hansen, C. Busse (RWTH Aachen)

Outline:

- Erosion of Pt (111)
- Growth of Al (111)
- grazing incidence bombardment:
  step-edge sputter yield
- Case study:
  Fluence dependent sputtering of Pt (111) by 5 keV Ar $\vartheta = 83^\circ$

Erosion of Pt (111)

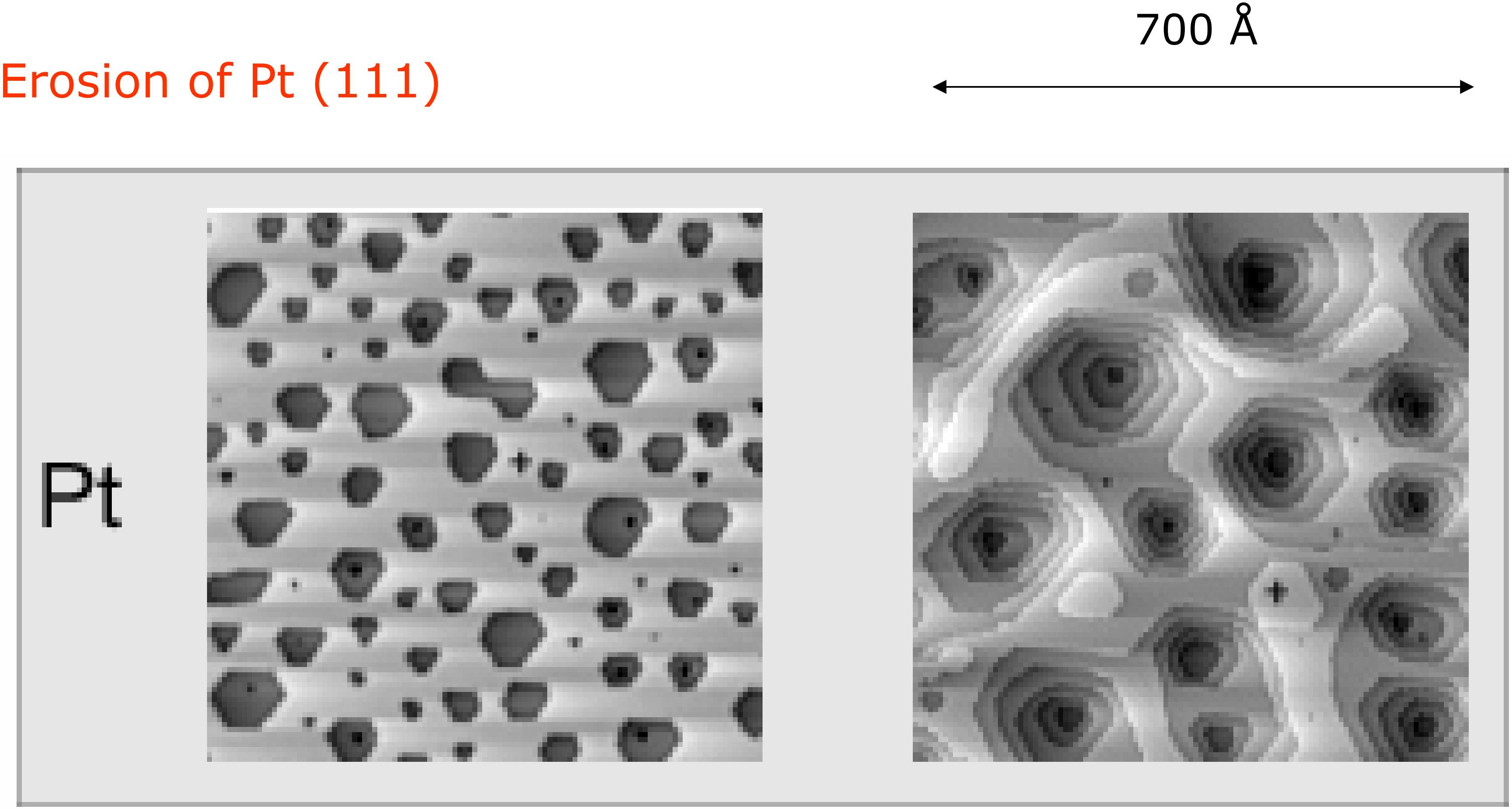

ion fluence:	0.09 ML	0.7 ML
erosion:	0.26 ML	2.1 ML

1 keV Xe -> Pt (111) @ 650 K
Busse et al. Surf Sci 488 (2001) 346

Formation of

Y_{ad} adatoms

Y_{sp} sputtered atoms

Y_{sv} surface vacancies

Y_{bv} bulk vacancies

Y_{i} interstitials

Conservation of mass:

$$Y_{sp} + Y_{ad} + Y_i = Y_{sv} + Y_{bv}$$

If diffusion possible:
bulk vacancies, interstitials,
(part of) surface vacancies anneal:
$Y_{sv,eff} = Y_{sp}$
(measurement of Y_{sp})

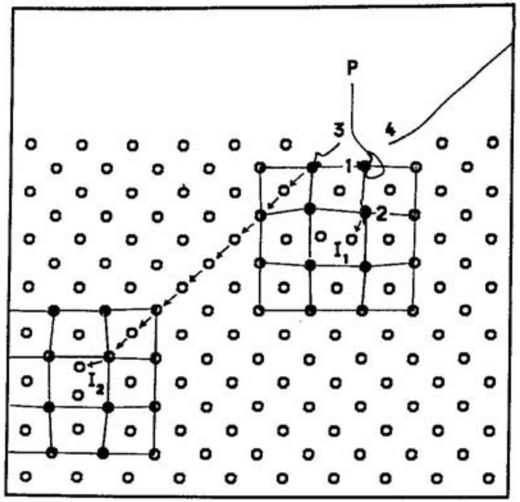

100 eV Cu → Cu
defects formed:
2 surface vacancies
2 interstitials
Karetta & Urbassek (1992)

Prediction from collision-cascade theory:

$$\frac{Y_{\mathrm{ad}}}{Y_{\mathrm{sp}}} = 2\frac{U_{\mathrm{sp}}}{U_{\mathrm{ad}}} - 1$$

where U_{sp}: energy dispensed to sputter an atom
U_{ad}: energy dispensed to lift an atom to adatom position

bond-counting argument:
Z=9 bonds of atom in fcc(111) surface plane
Z=3 bonds adlayer

pair potentials: $U_{sp}/U_{ad} = 9/6$ $Y_{ad}/Y_{sp} = 2$

many-body: $$\frac{Y_{\mathrm{sp}}}{Y_{\mathrm{ad}}} = \frac{\sqrt{9}}{\sqrt{9} - \sqrt{3}}$$ $Y_{ad}/Y_{sp} = 4$

Conclusions:
PR B 50 (1994) 11167

- rough quantitative agreeement of expt and simul
- $Y_{ad}/Y_{sp} \cong 4$
- at low energy: deviations due to steeper energy spectrum

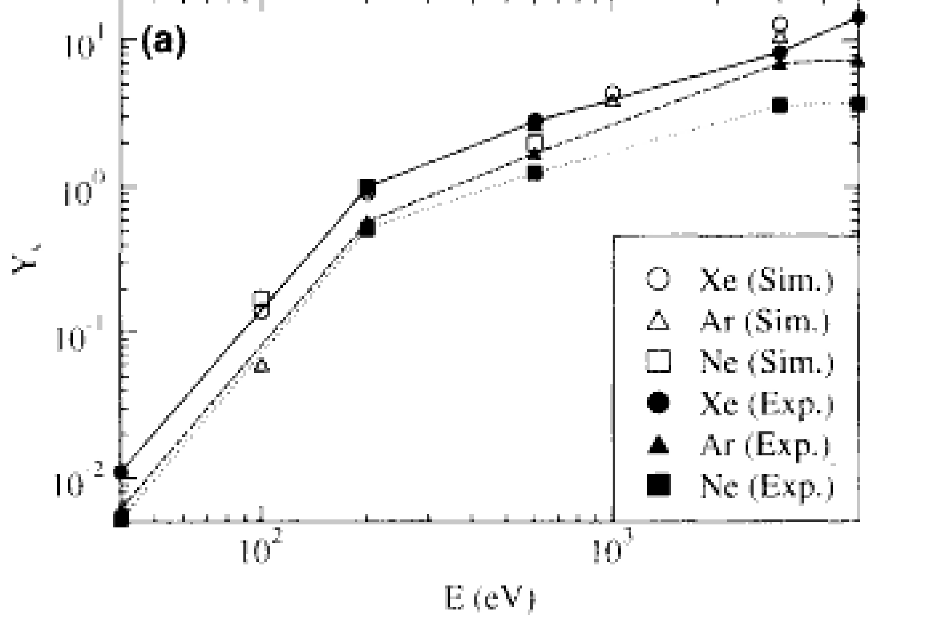

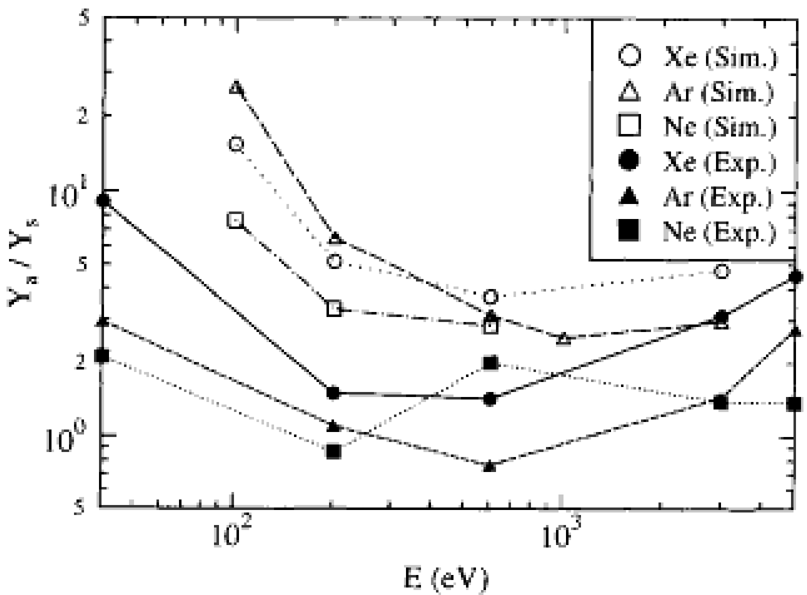

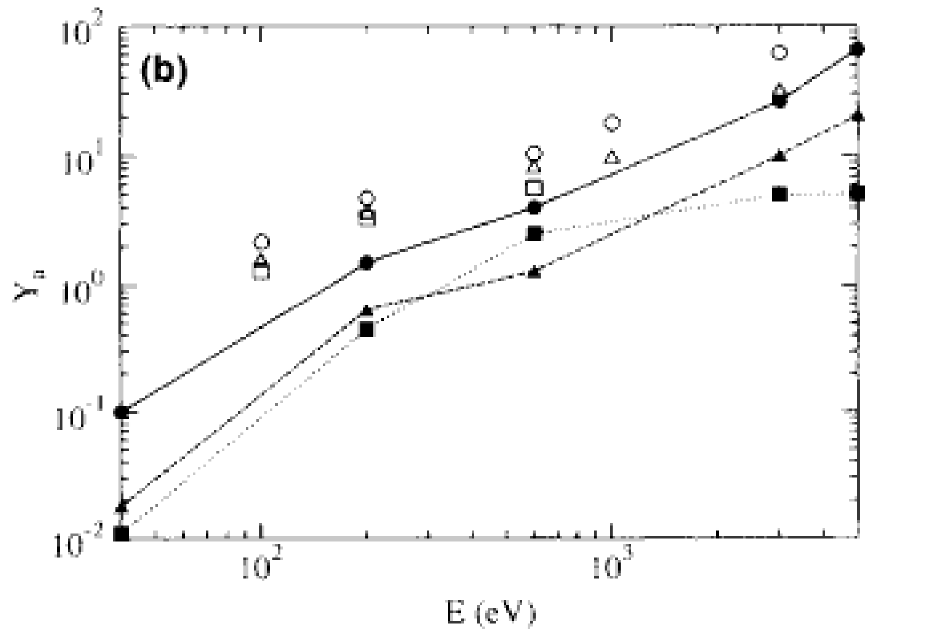

Growth of Al (111):

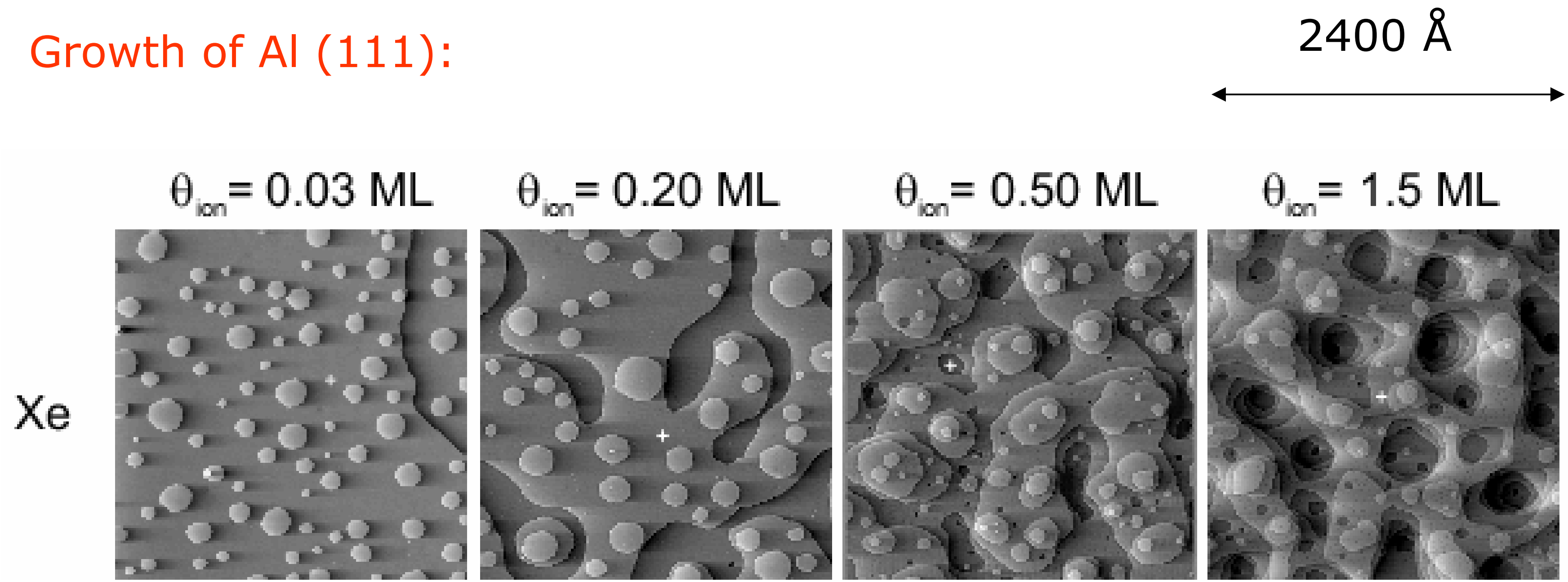

ion fluence: 0.03 ML 0.20 ML 0.50 ML 1.5 ML

net growth net erosion

1 keV Xe -> Al (111) @ 300 K
(+) marks height of original surface
Busse et al. Surf Sci 488 (2001) 346

Experiment and MD simulation:

- preponderance of adatom over surface vacancy formation
- spike-induced local melting
- outflow of liquid (swelling)
- rapid resolidification -> amorphous zones hinder diffusion
- formation of vacancy clusters: hinders diffusion

Preponderance of adatom over surface vacancy formation

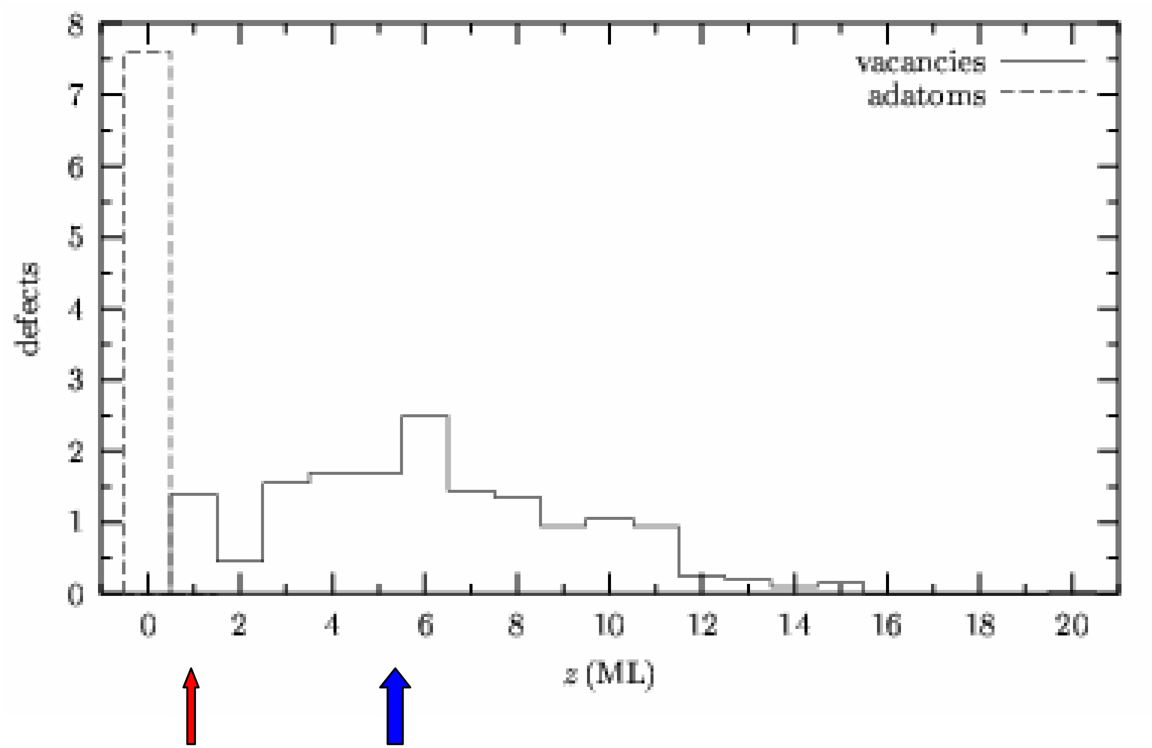

Surface vacancies
separated from bulk vacancies

Formation of vacancy clusters: hinders diffusion

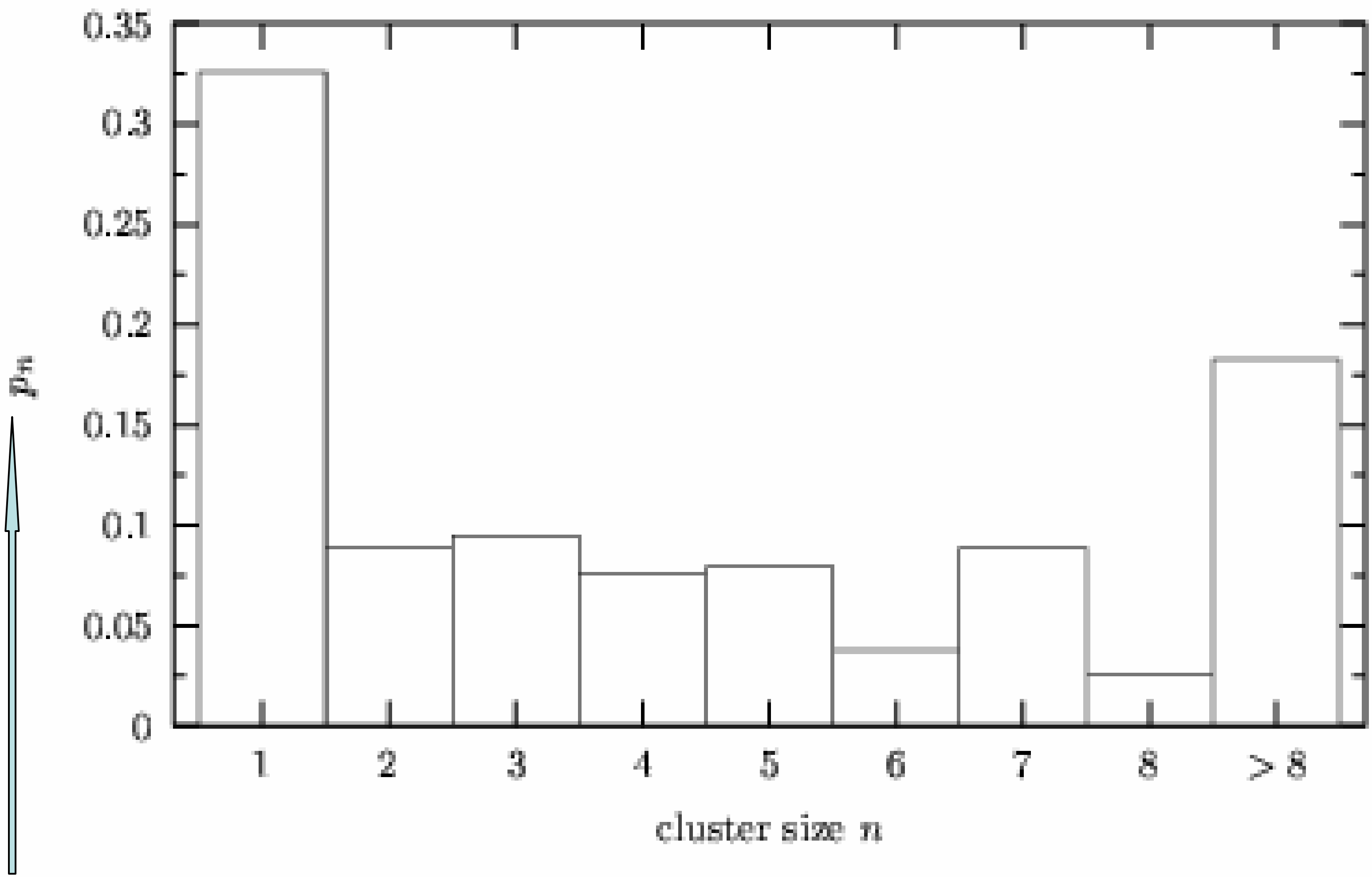

Probability that a vacancy is part of a vacancy cluster of n vacancies

Outflow of liquid (swelling):

prompt (ballistic)   delayed (thermal spike)

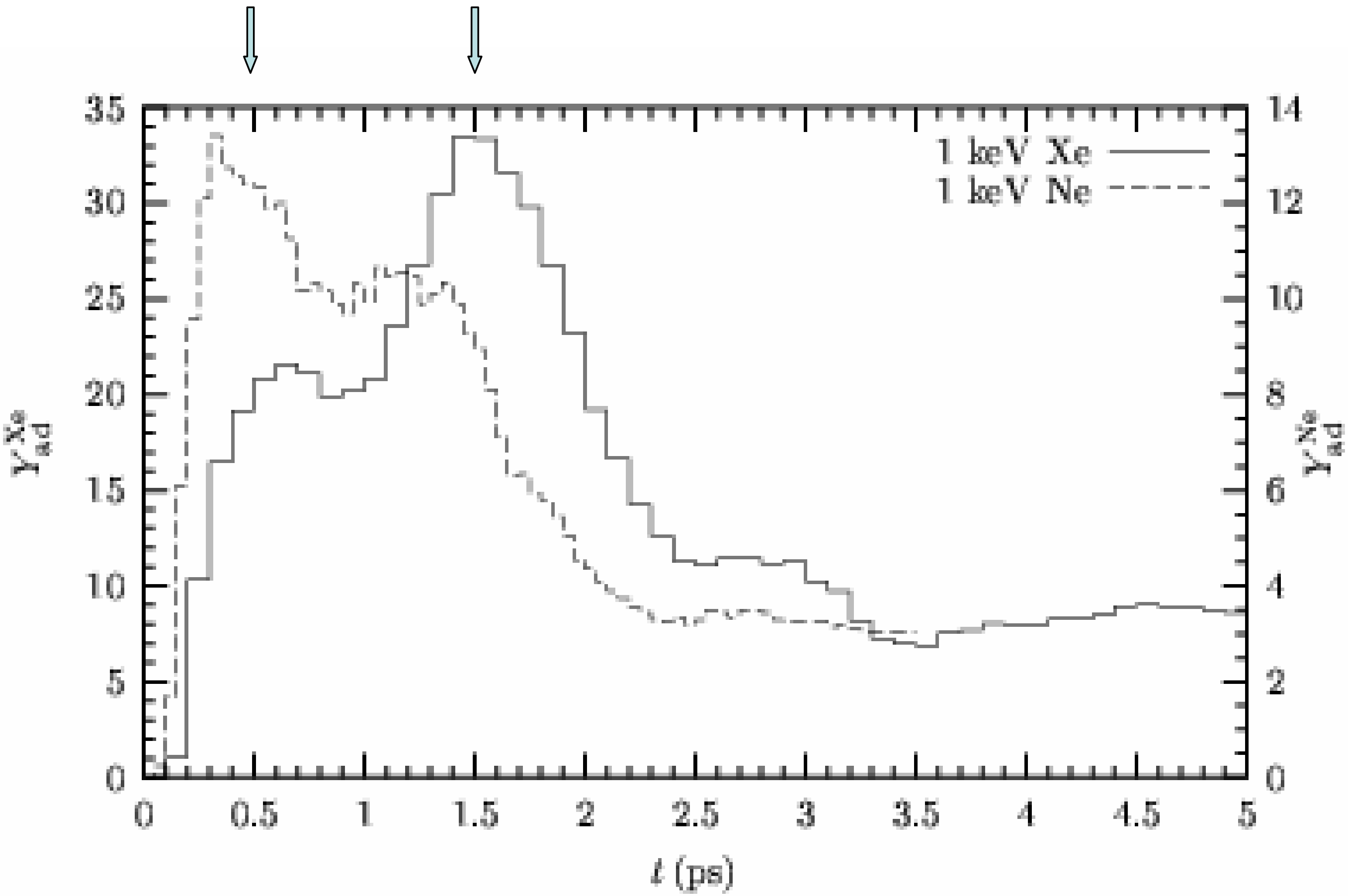

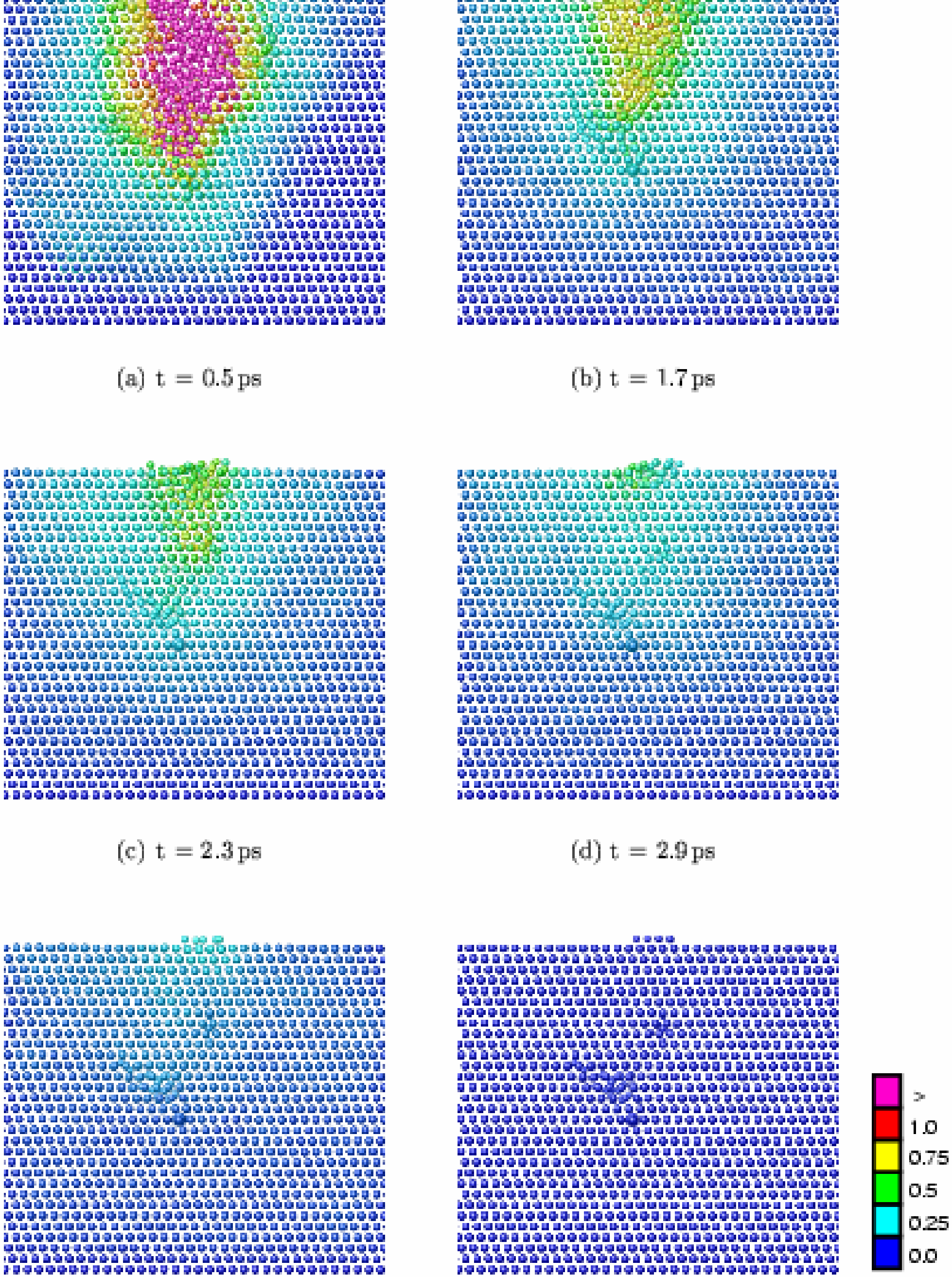

(a) t = 0.5 ps (b) t = 1.7 ps

(c) t = 2.3 ps (d) t = 2.9 ps

(e) t = 4.1 ps (f) t = 15.0 ps

outflow of liquid (swelling)
rapid resolidification
→ amorphous zones

movie

1 keV Ne impact
for comparison:

no swelling
no amorphization

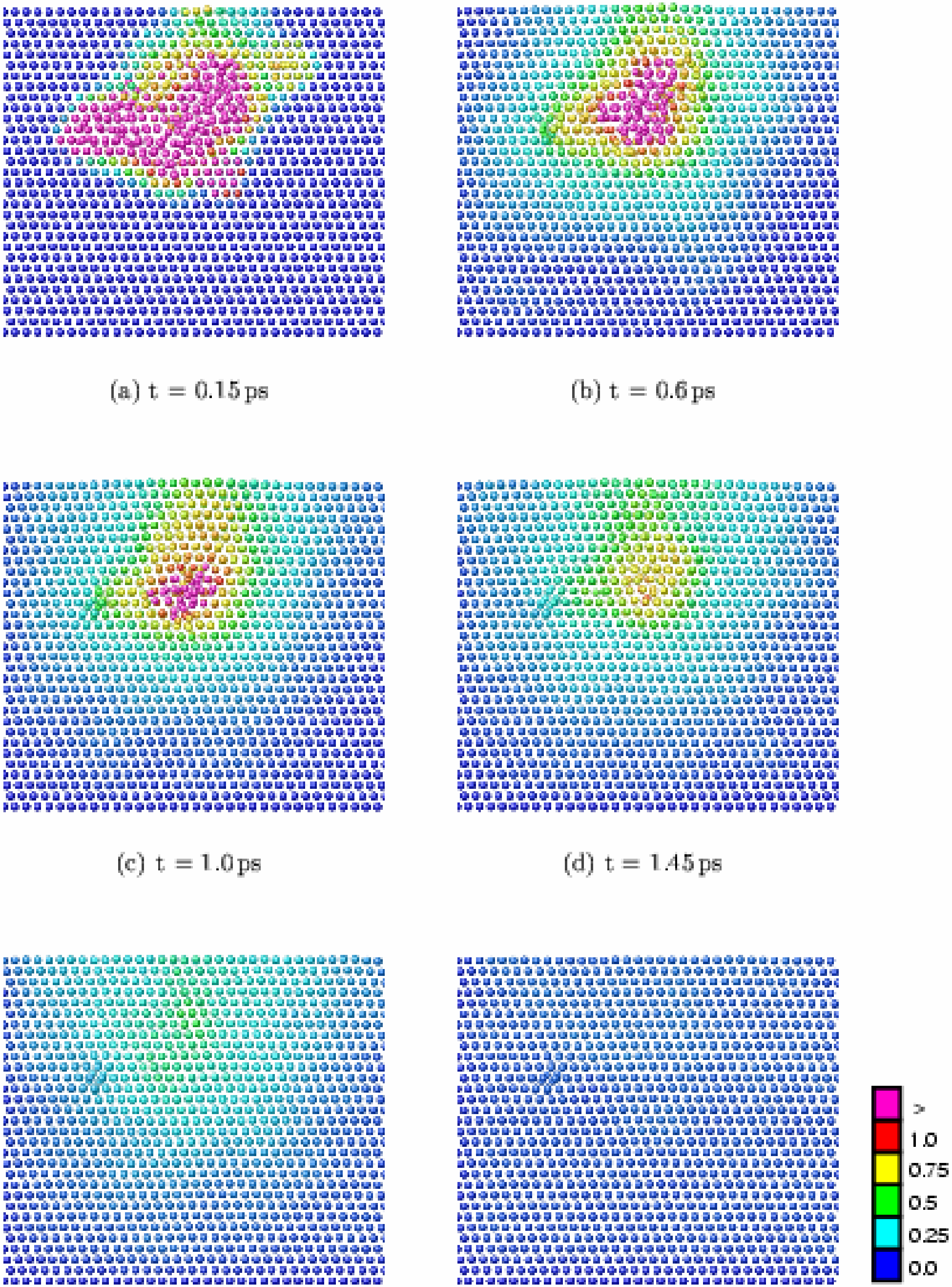

(a) t = 0.15 ps

(b) t = 0.6 ps

(c) t = 1.0 ps

(d) t = 1.45 ps

Top views:

Preponderance of adatom over surface vacancy formation

- surface atom
- adatom
- ion (impact point)

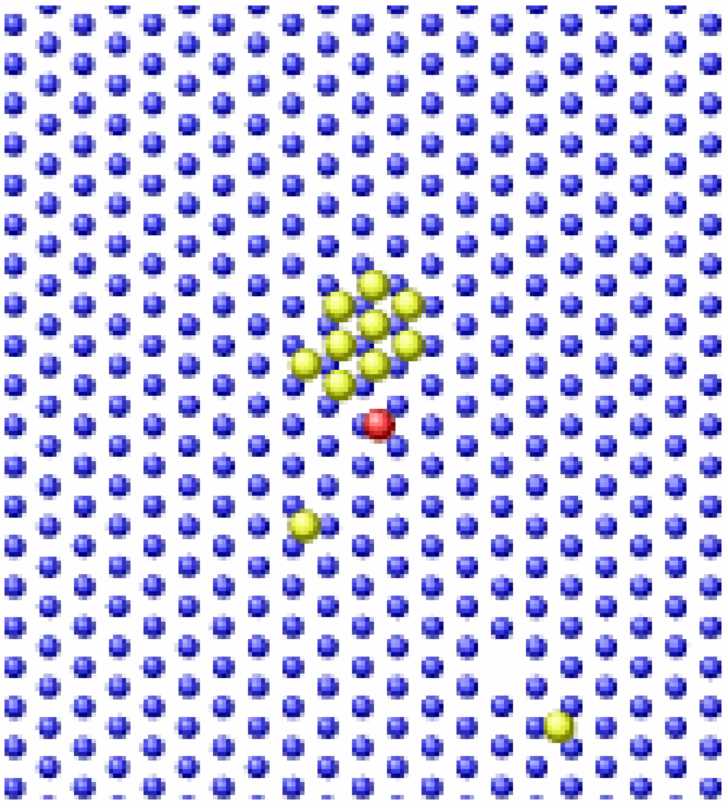

(a) 1 keV Xe^+

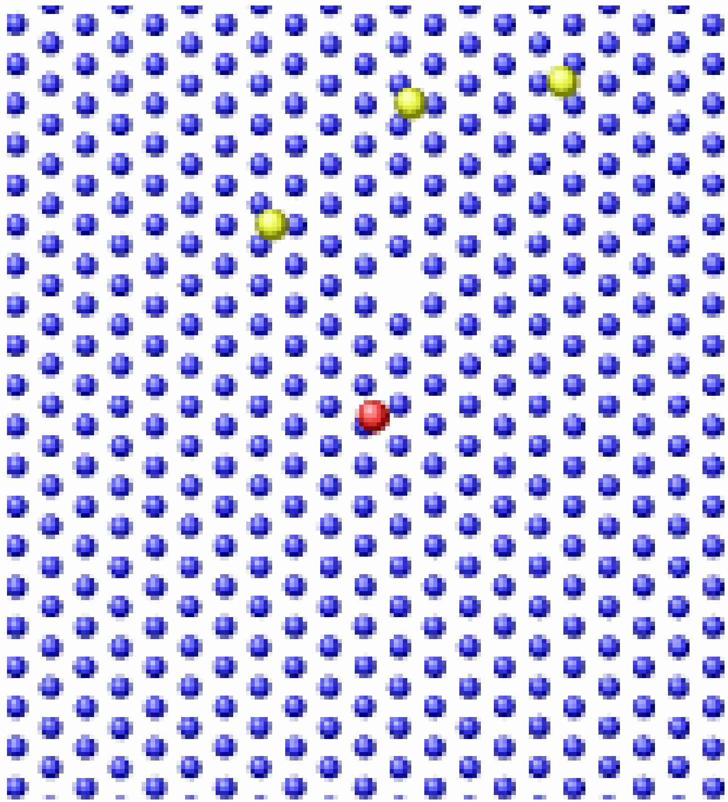

(b) 1 keV Ne^+

Experiment and MD simulation:

- preponderance of adatom over surface vacancy formation
- spike-induced local melting
- outflow of liquid (swelling)
- rapid resolidification -> amorphous zones hinder diffusion
- formation of vacancy clusters: hinders diffusion

Grazing incidence bombardment: step-edge sputter yield
Surf Sci 547 (2003) 315

5 keV Xe $\rightarrow$ Pt (111)
B-step = {111} micro-facetted step = along [1-1 0] direction
ion impact along [-1 -1 2]

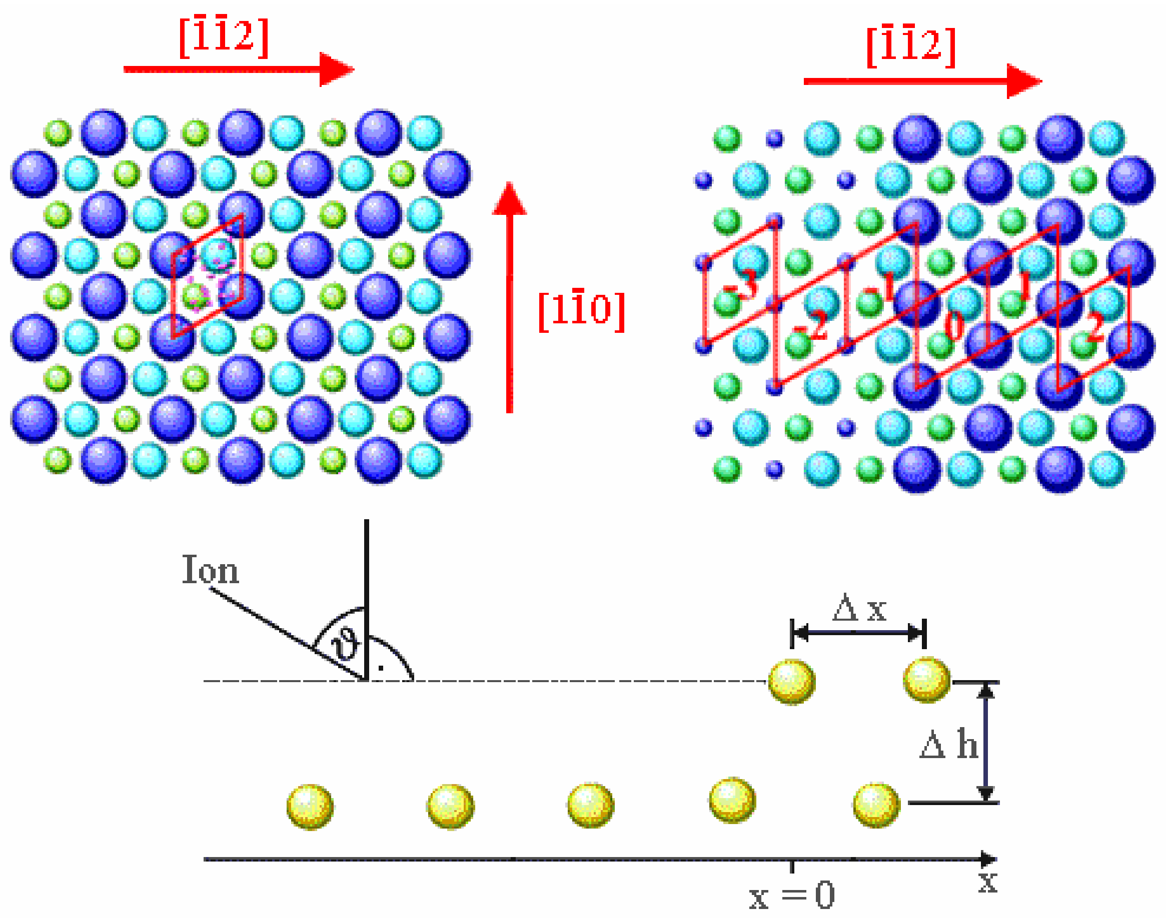

ion impact
$\xi = x / \Delta x$

Flat terrace: Y_{sp}, Y_{ad} = 0 for $\vartheta \geq 80^{\circ}$
Near Step (ξ=-1): substantial sputtering and damage

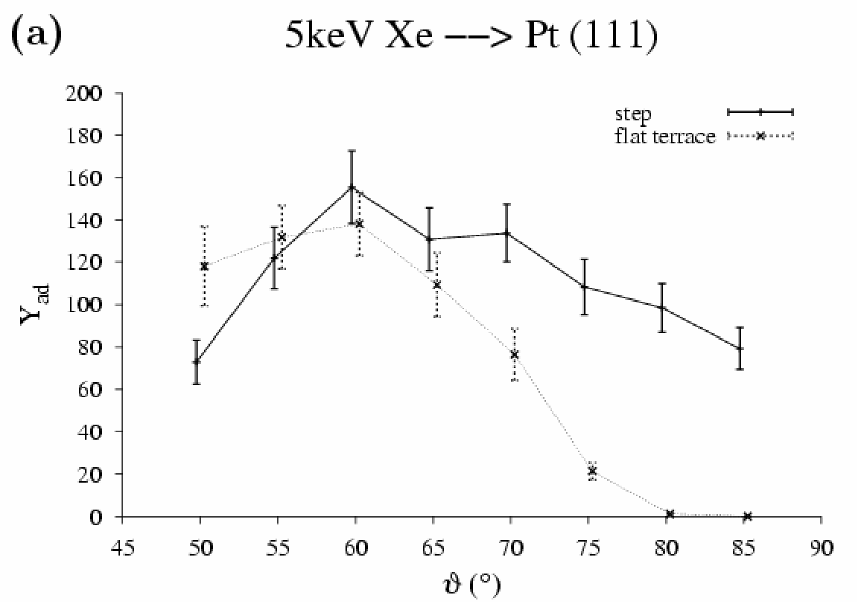

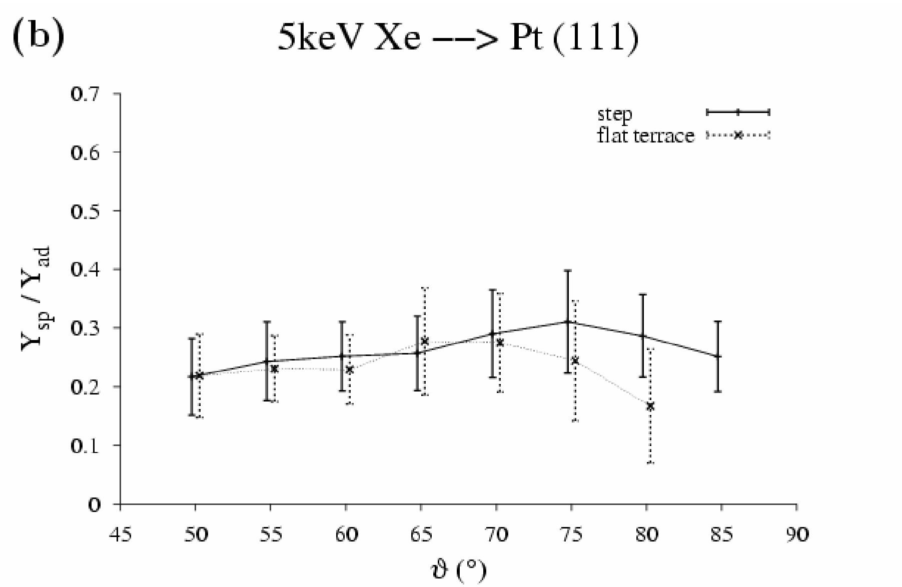

$Y_{ad}/Y_{sp} \cong 4$

Dependence of damage and sputter yield on distance ξ to step roughly a rectangular function

Y_{ad} = const. for $-x_c < \xi < 0$

$x_c = 2 \Delta h \tan \vartheta$: distance where ion reflects clear from the step

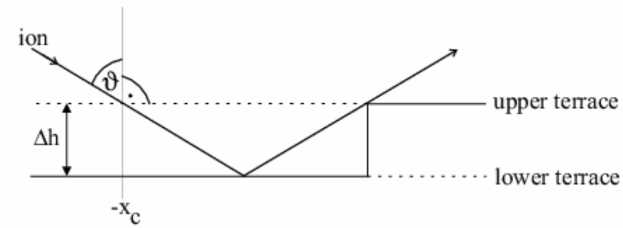

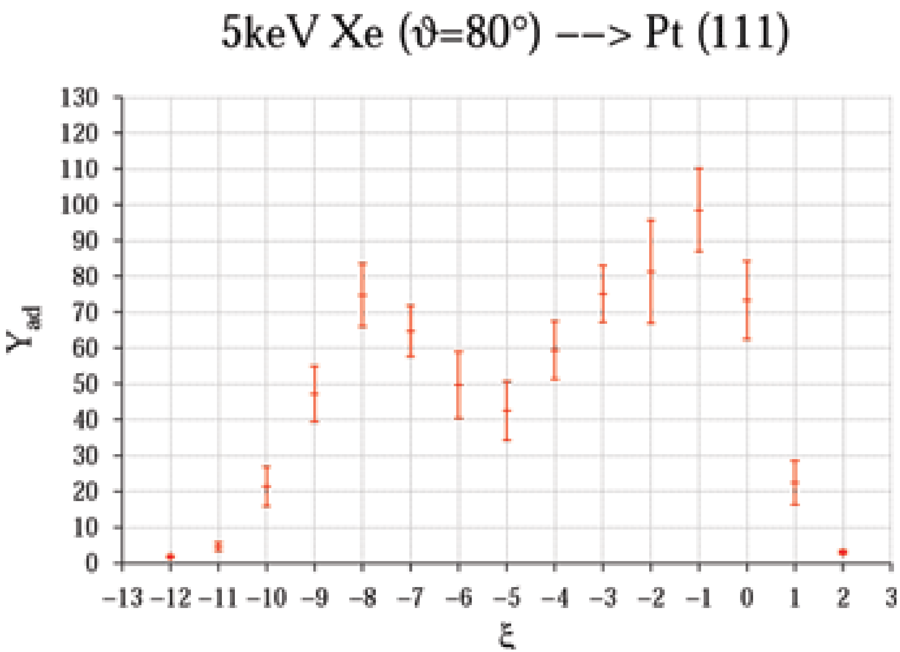

Top views, $\vartheta = 80^{\circ}$ (ξ=-1):

average event: $Y_{ad} = 126$

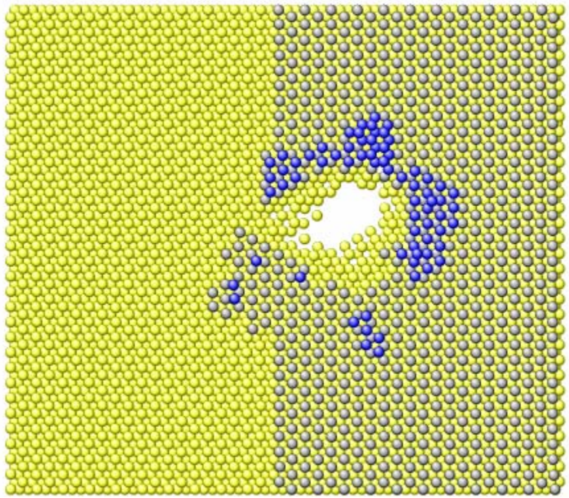

productive: $Y_{ad} = 169$

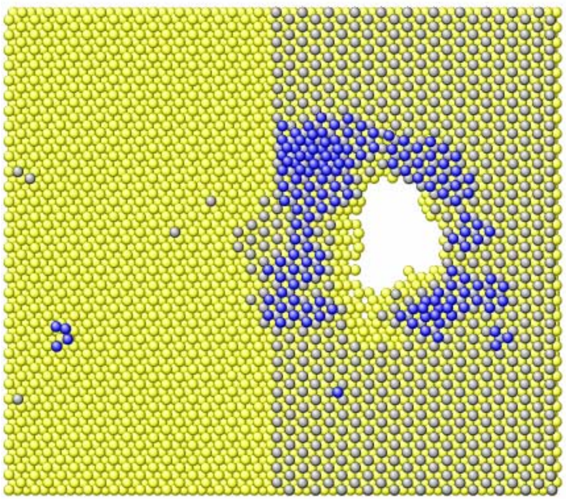

poor: $Y_{ad} = 34$

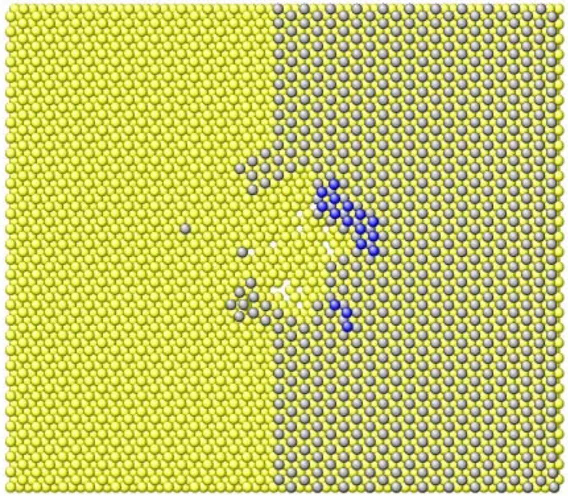

Beschuss der flachen Terrasse in einem Polarwinkel von 80°
Beschuss der B-Stufe in einem Polarwinkel von 80° in Zelle $\xi = -1$
Beschuss der B-Stufe in einem Polarwinkel von 80° in Zelle $\xi = -9$
Beschuss der B-Stufe in einem Polarwinkel von 80° in Zelle $\xi = -11$

Conclusions: 5 keV Xe -> Pt (111)

- Flat terrace: Y_{sp}, Y_{ad} = 0 for $\vartheta \geq 80^\circ$
- Near Step: substantial sputtering and damage
- Dependence of damage and sputter yield on distance ξ to step roughly a rectangular function
- influence of step reaches a distance $x_c = 2\,\Delta h \tan\vartheta$ before the step
- damage preferentially produced on upper terrace (behind step)
- step edge smears out

Case study: prl 92 (2004) 246106

Fluence dependent sputtering of Pt (111) by 5 keV Ar at $\vartheta = 83^{\circ}$

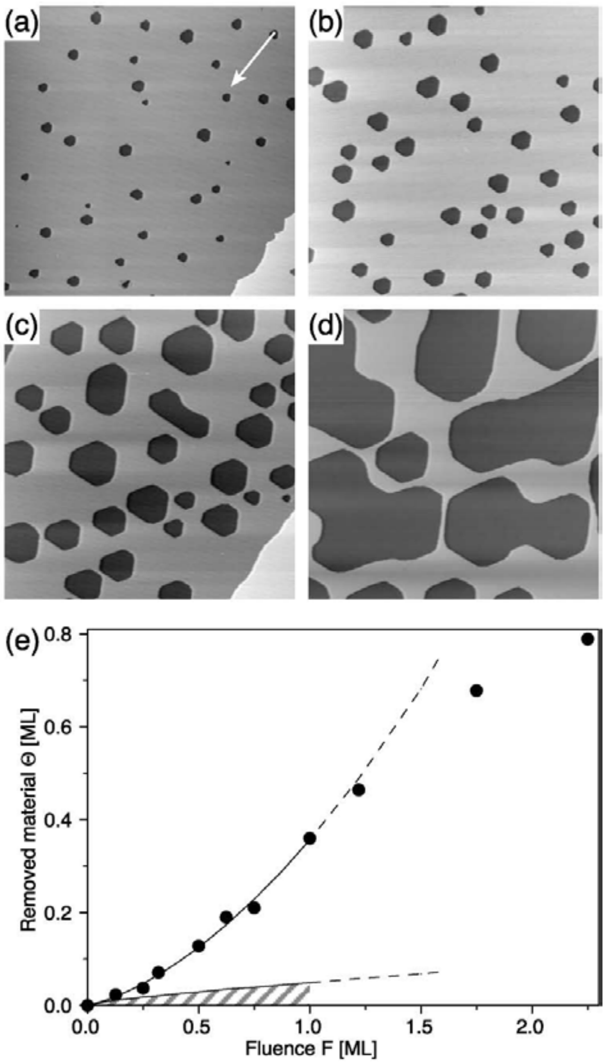

2450 Å

STM topographs at ion fluences of F= 0.25, 0.5, 1.0, 1.75 ML @ 720 K

Removed material vs fluence.
Line: model
Hatched: sputter yield of terraces

Interpretation:

$$Y = Y_{step} \cdot A_{step} + Y_{terrace} \cdot (1 - A_{step})$$

Y_{step}	average yield in front of steps
$Y_{terrace}$	average yield of terraces
A_{step}	area fraction of island impact areas

Fit of Y(F) yields:

Y_{step}	$= 8.4 \pm 1.5$	MD: 8.3
$Y_{terrace}$	$= 0.08 \pm 0.03$	MD: 0

Note:

For A_{step} use

$d \cdot x_c$	if island diameter	$d > x_c$
A_{island}	if	$d < x_c$

At large fluence F, island coalescence decreases sputter yield

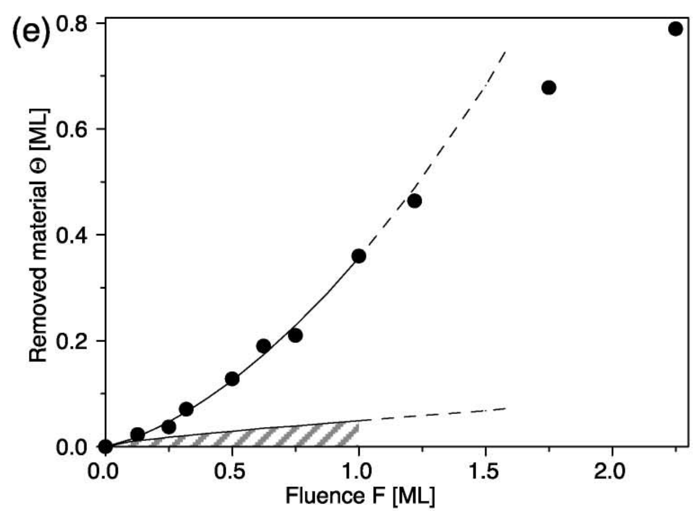

Cluster-induced cratering: linking nano- and microscales

Chr. Anders, St. Zimmermann, H. M Urbassek

Physics Dept., University of Kaiserslautern, Germany

E. Bringa

Lawrence Livermore Natl Labs, CA

Thanks to: R. E. Johnson (Univ Virginia)

Cluster-surface interaction:

- materials production:
  - cluster deposition of materials
  - thin-film growth
    crystalline nuclei, increased adatom mobility
- surface technology:
  - surface modification
  - surface cleaning
  - soft landings: preparation of supported clusters
  - surface smoothing (by lateral cluster spreading)
- planetary sciences
  - solar wind, dust, ... impact -> surfaces of icy moons, comets etc
  - collisions within planetay ring systems
  - dust analysis by spacecraft: CASSINI, STARDUST

cluster deposition of materials

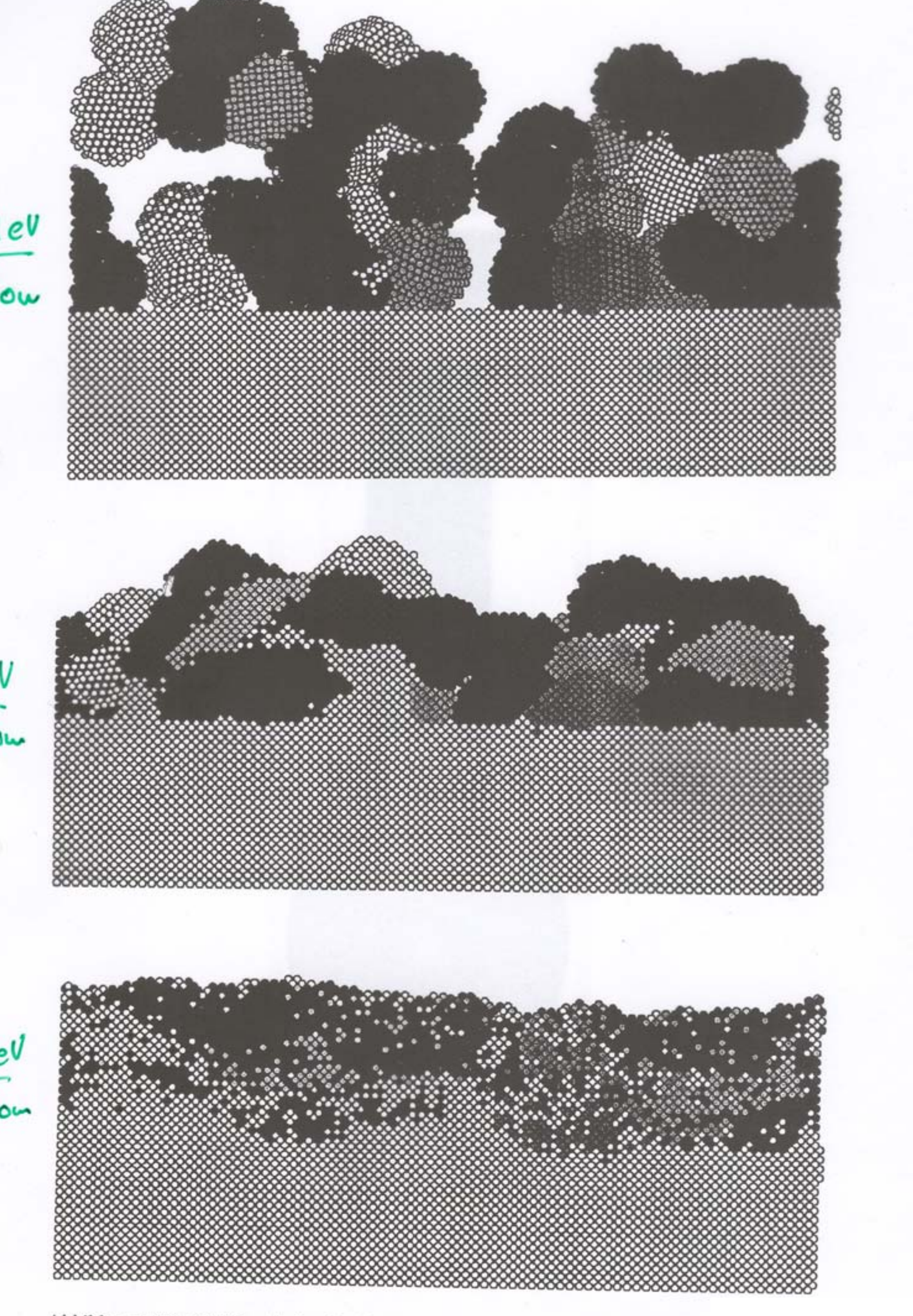

Moseler 1993

15 km

nucleus of comet Halley
Giotto (1986)

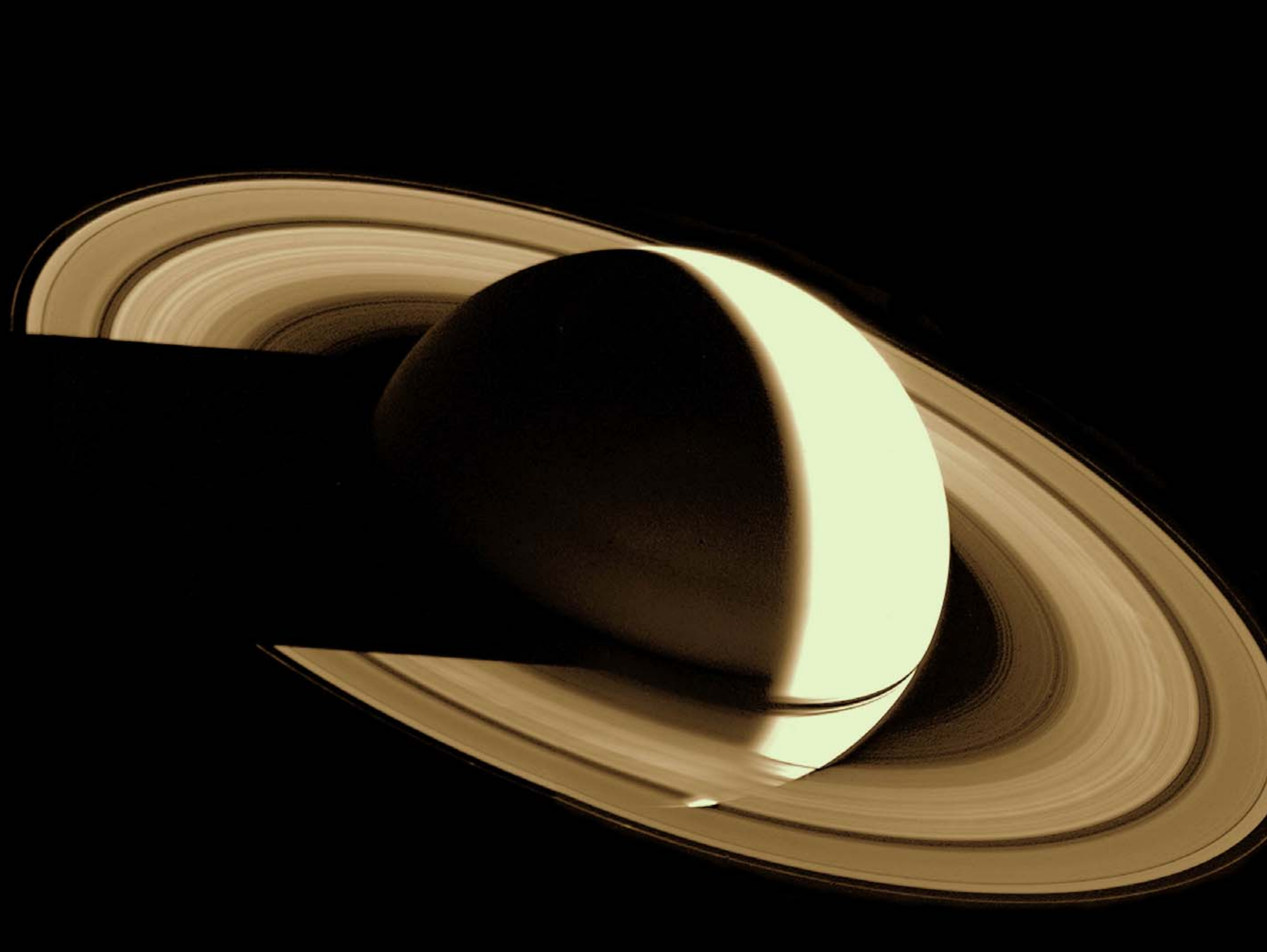

dust grain (20 μm)
collected by airplane

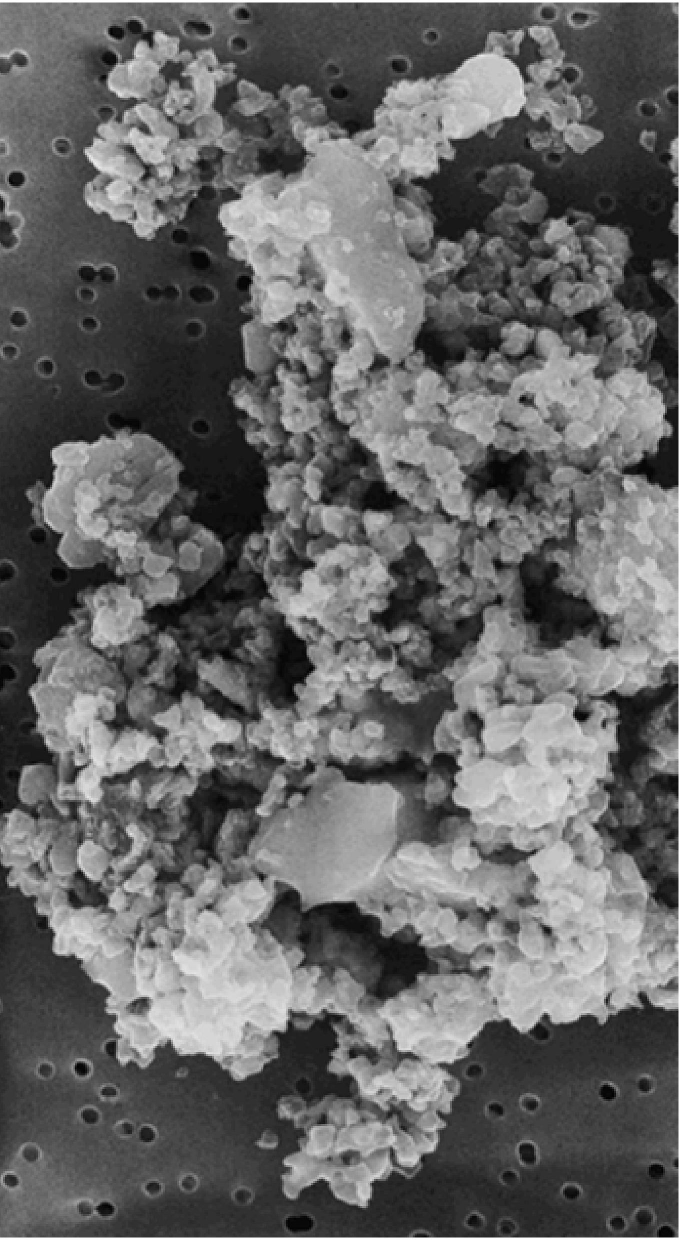

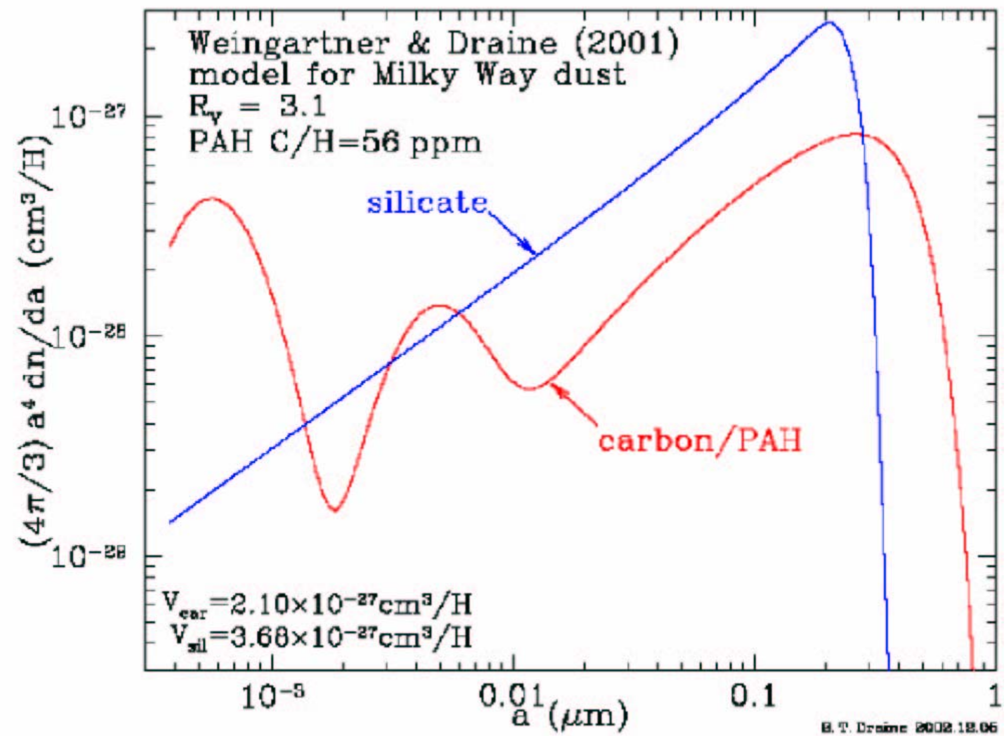

dust analysis
on the
CASSINI mission

Abb. 1: Die Raumsonde CASSINI/HUYGENS während der Endmontage in Cape Canaveral. Oben ist die in Italien gebaute Hauptantenne zu sehen, links die HUYGENS-Sonde, direkt darüber der in Heidelberg entwickelte Staubdetektor »Cosmic Dust Analyzer« (CDA), unten die beiden Haupttriebwerke, rechts die Fernerkundungsinstrumente einschließlich der beiden Kameras, die vom Betrachter wegblicken.

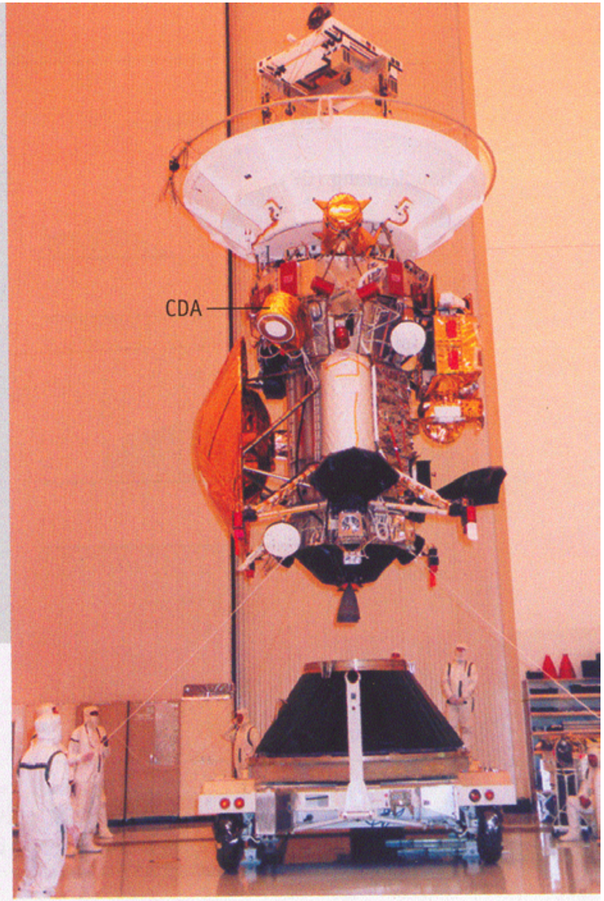

Abb. 2: Der Cosmic-Dust-Analyzer eingepackt in Thermalisolationsfolie. Das runde Detektorgehäuse hat einen Durchmesser von 40 cm. Im Gehäuse sieht man die Eintrittsgitter und die Streben des Multipliergehäuses. Die beiden runden Folienflächen gehören zum High-rate-Detektor. Zur Ausrichtung in die Staubrichtung besitzt das Experiment einen Drehtisch (unten).

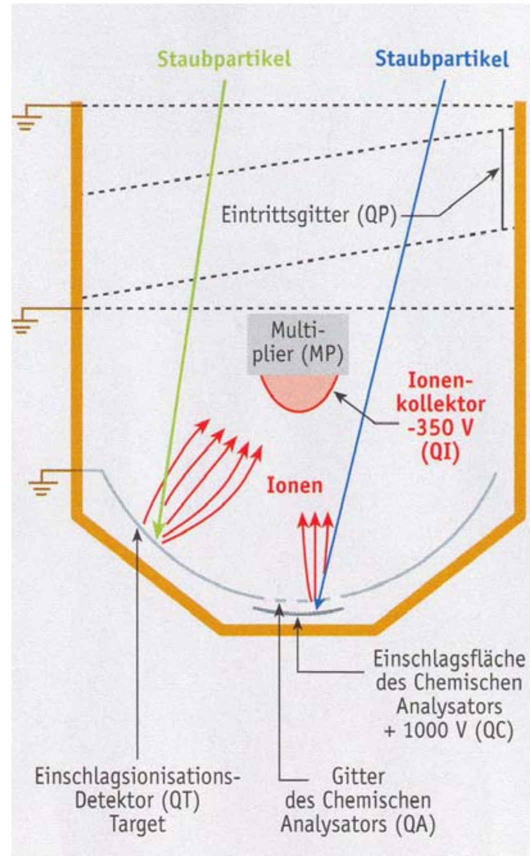

ΣυΩ 09/04

Outline:

I. Craters at the nano-, micro-, macroscale

II. Crater simulations by molecular dynamics

A) Cratering: systematic results for Ar system

B) Cratering: pictorial results for Cu system

III. Comparison to experiment

I. Craters at the nano-, micro-, macroscale

- nano: cluster impacts
- micro: dust particles
- macro: (micro-) meteorites, ...

Cratering experiments at the nanoscale:

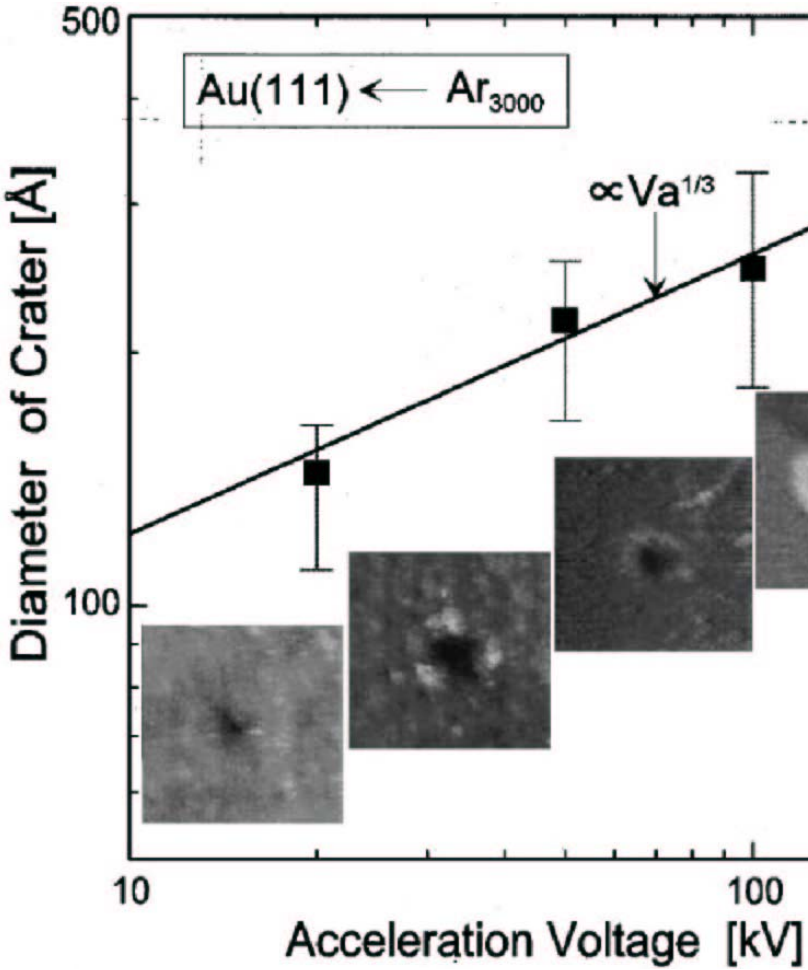

Yamada, Insepov et al

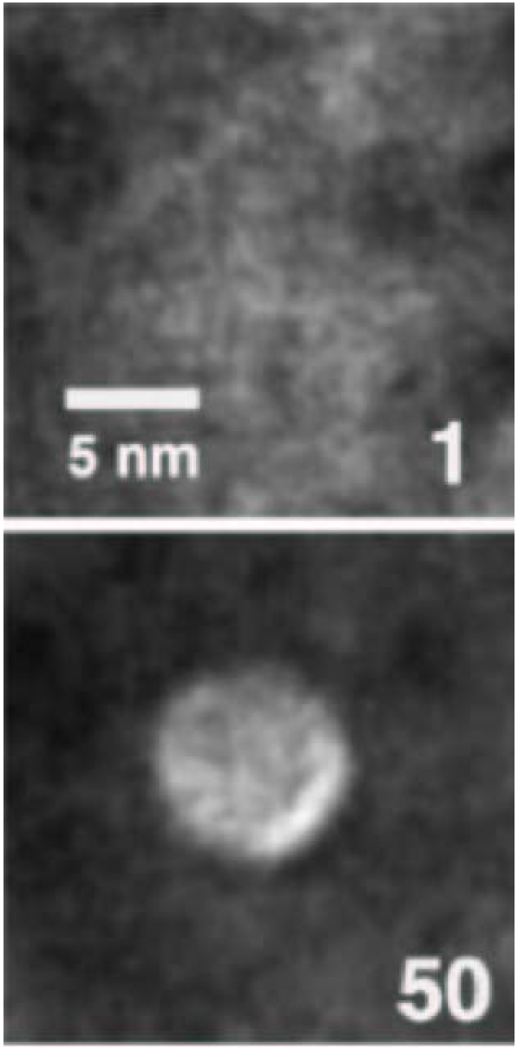

Xe -> Au:
Donnely & Birtcher

Craters at the microscale: metal projectiles (d = 0.1 – 5 µm)

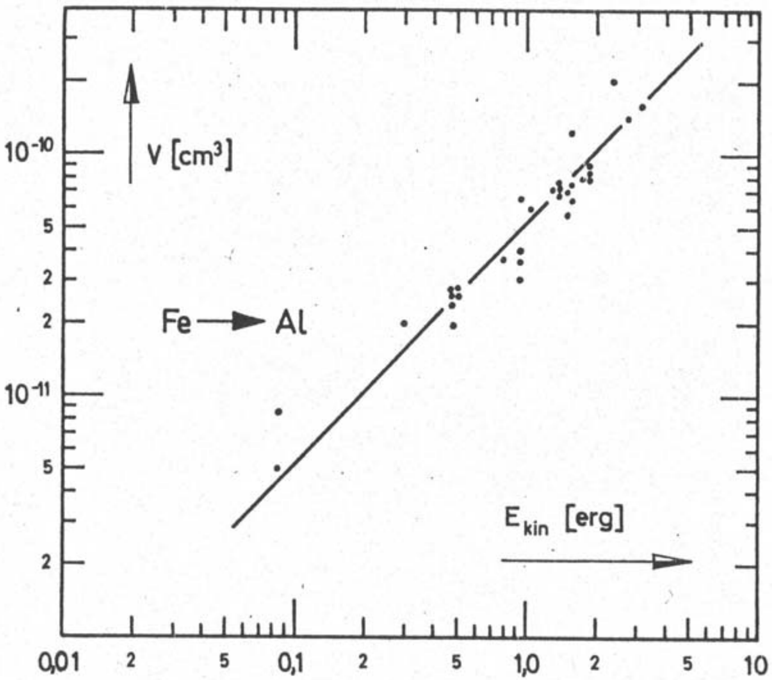

Abb. 9. Das eigentliche Kratervolumen $V(T')$ in Al als Funktion der Projektilenergie E_{kin}. Die Meßpunkte entsprechen verschiedenen Projektilmassen und verschiedenen Projektilgeschwindigkeiten (für $v > 1$ km/sec).

Rudolph, Z Naturforsch 24a (1969) 326

K. Eichhorn and E. Grün: High-velocity impacts of dust particles

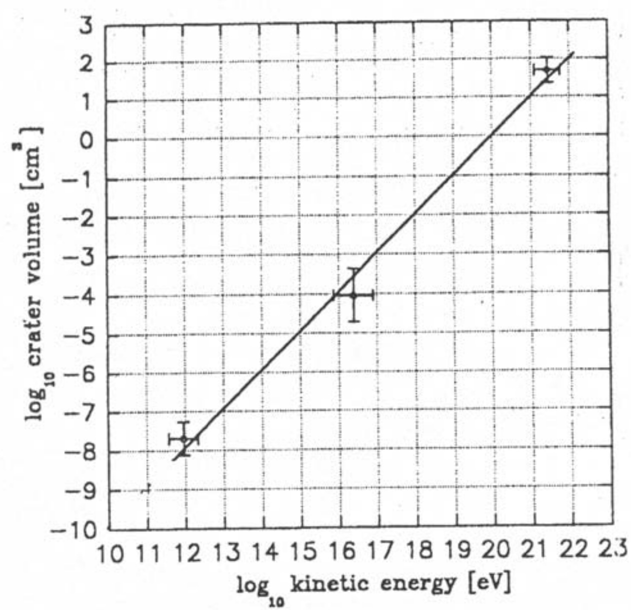

Fig. 6. Crater volume vs kinetic energy from different experiments. The current experiment is the data point at 10^{12} eV, at 10^{16} eV the data from Frisch (1992) and at 10^{22} eV the data from Lange and Ahrens (1987). Each data point is the average value of all data points from the author. The error bars represent the standard deviation

$$V(E_{\text{kin}}) = 2.34 \times 10^{-20} E_{\text{kin}}^{0.98}.$$

Planet Space Sci 41 (1993) 429

Craters at the microscale

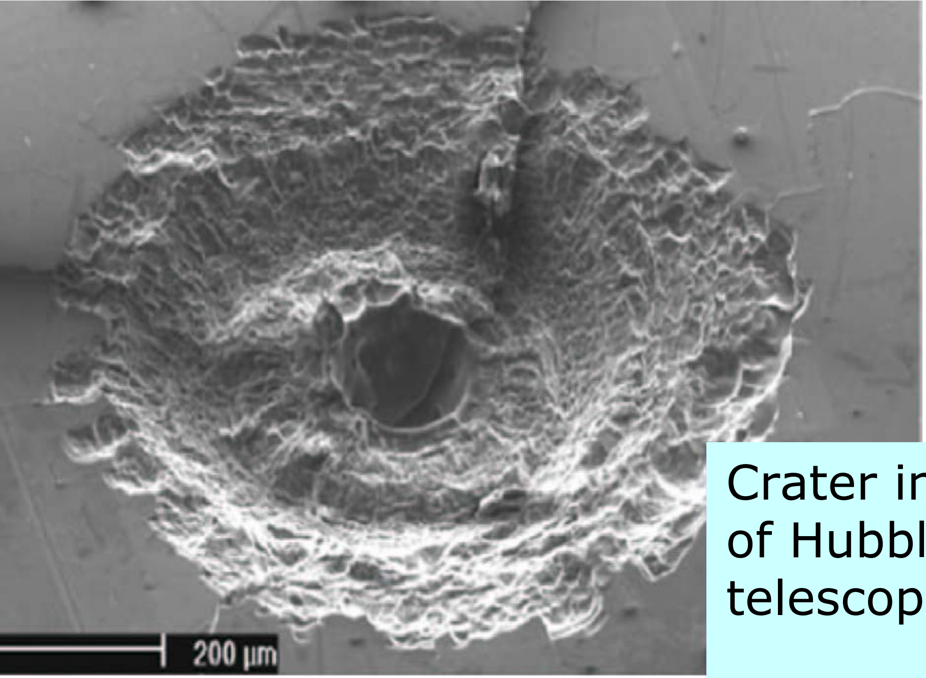

Crater in solar cell of Hubble space telescope

Graham et al, Int J Impact Eng 26 (2001) 263

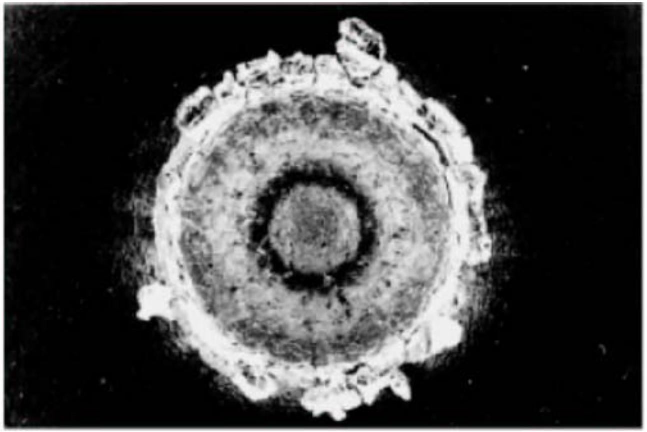

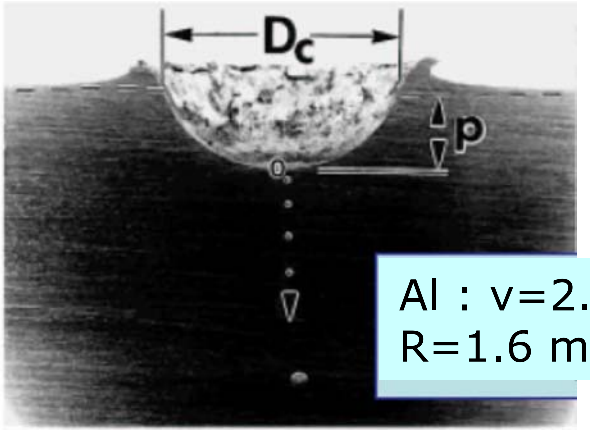

Al : v=2.6 km/sec, R=1.6 mm -> Cu

Quinones & Murr, Phys Stat Sol A 166 (1998) 763

Cratering experiments at the macroscale:

Barringer-Krater, Arizona: 1200 m Durchmesser, 200 m tief
entstanden vor 50 ka durch 50m-Meteorit

Gaspra
Galileo-Beiflug in
1200 km Entfernung
19 x 12 x 11 km

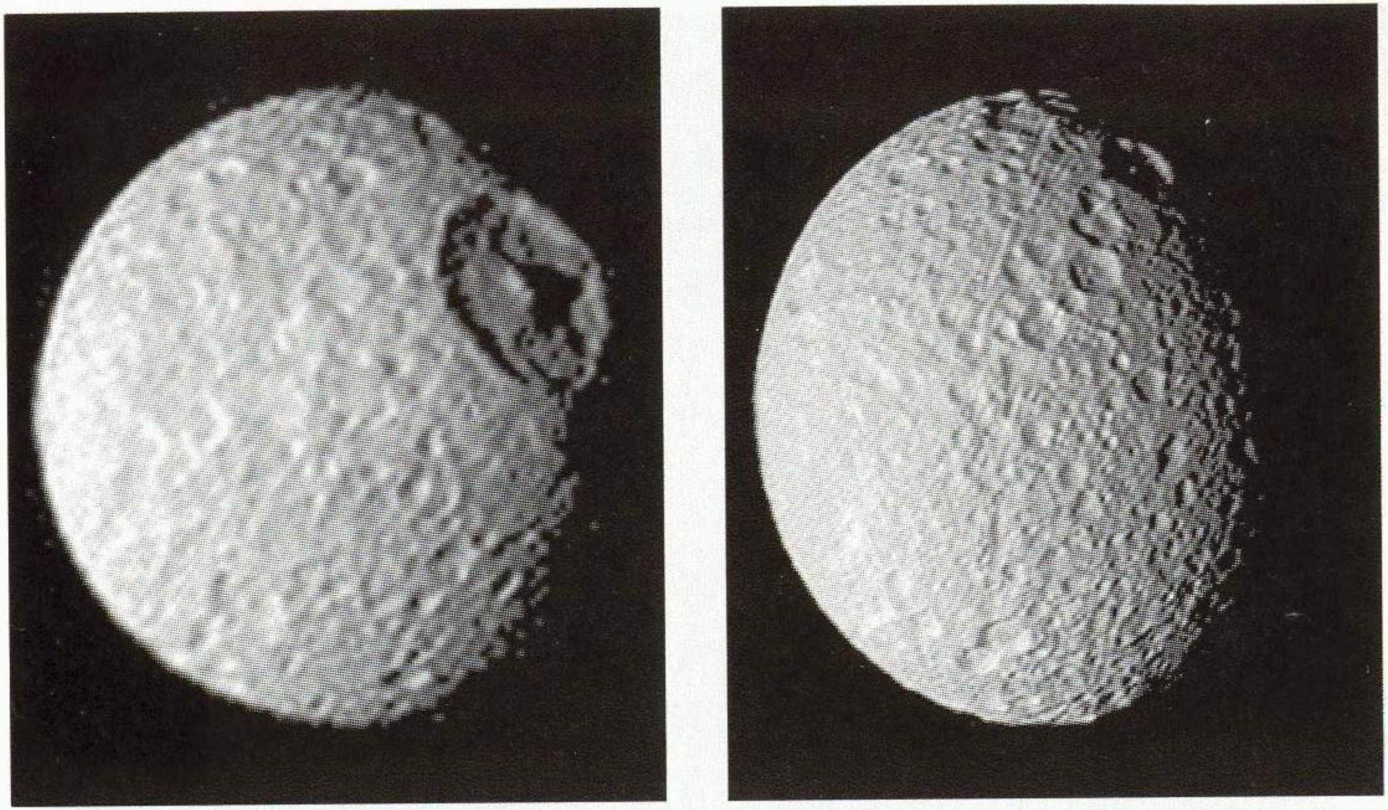

Figure 3. Voyager 1 images of crater-pocked Mimas reveal two different hemispheres of this inner, 400-km-diameter satellite of Saturn. Craters are spaced closely and overlap each other, indicating that the surfaces seen are ancient. The relatively large, 130-km-diameter crater Herschel is named after Mimas's discoverer. Several fissures or grooves (best seen in the right image) may be a consequence of Herschel's formation, heat-driven expansion of the crust, or tidal forces from Saturn.

Βεαττψ

Crater morphologies
diameters are for Moon
(approximate)

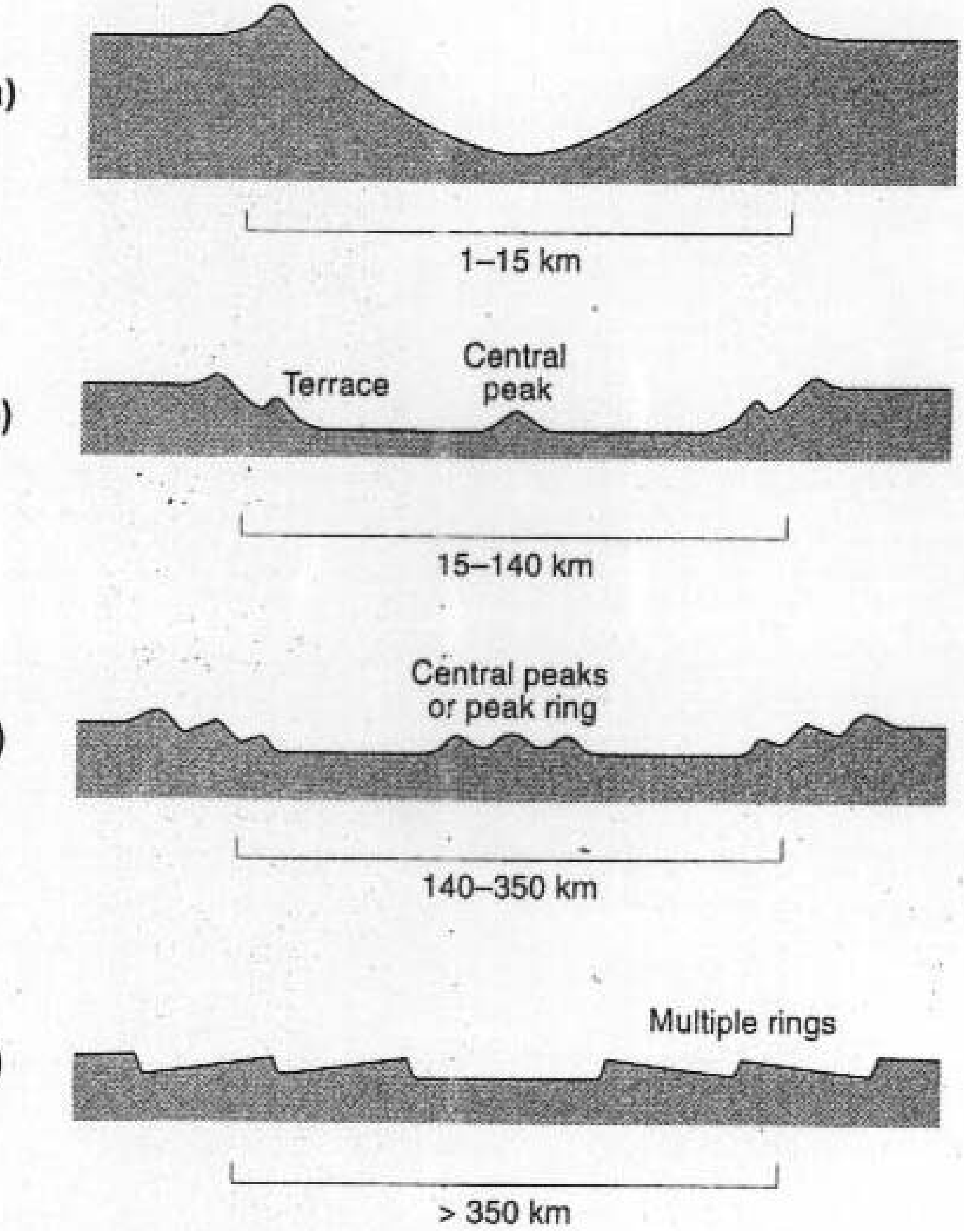

Copernicus

Jones

II Crater simulations by molecular dynamics

Notation:

- E total cluster energy
- E/n impact energy / projectile atom
- Y total sputter yield
- Y/n sputter yield / projectile atom

- U cohesive energy
- $\varepsilon = E/U$ scaled cohesive energy

Cratering simulations by MD:

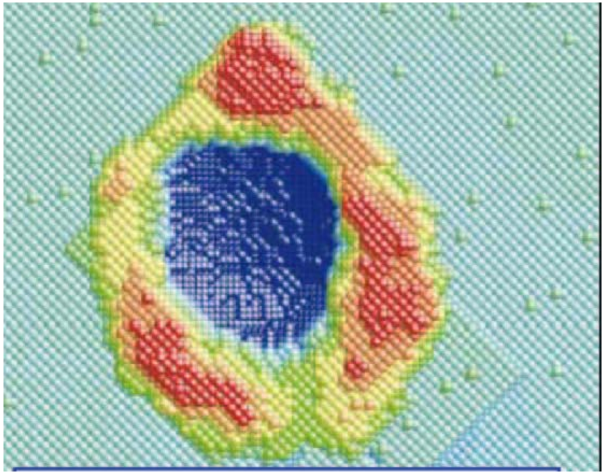

100 keV Xe_1 -> Au
Bringa & Nordlund

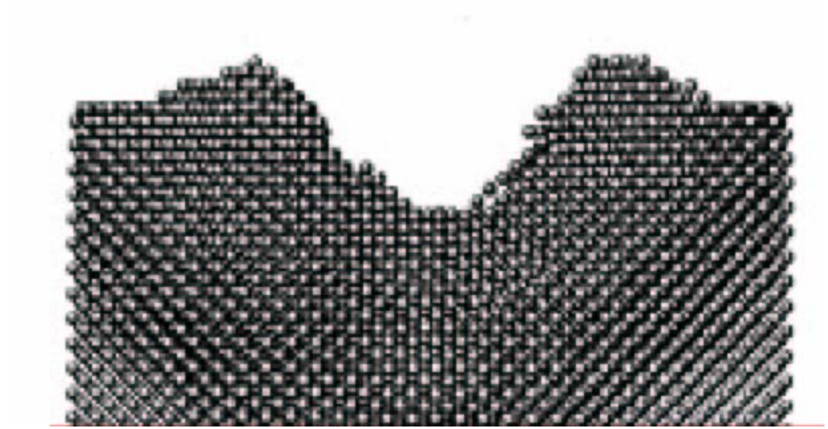

10 keV Cu_{13} -> Cu
Aderjan & Urbassek

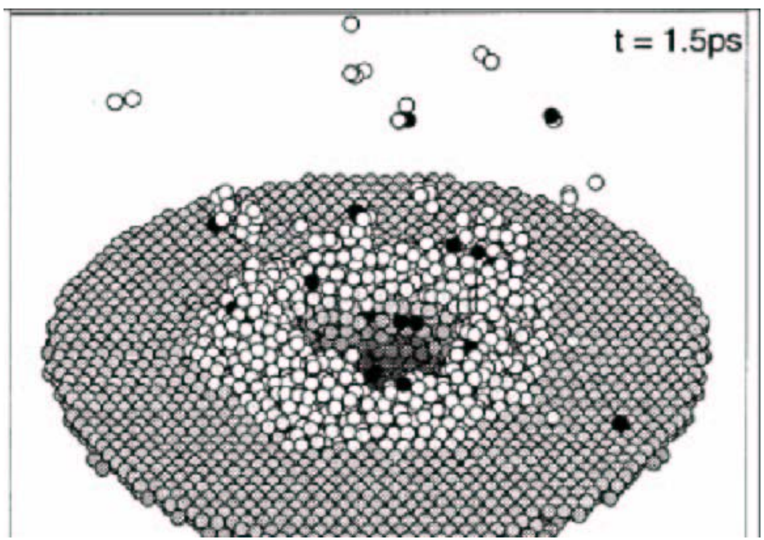

5.5 keV Cu55 -> Cu
Muramoto & Yamamura

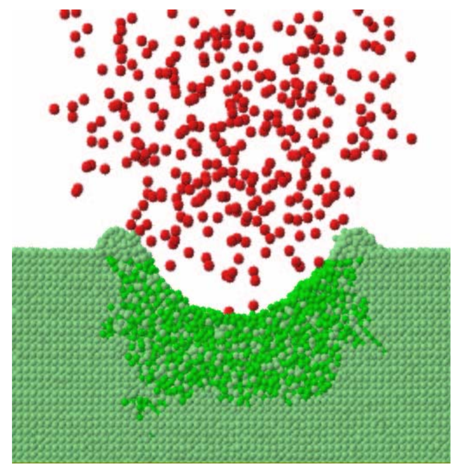

20 keV Ar_{2000} -> Si
Aoki et al.

Interest

Here:

- sputter yield Y
- crater size V

Further:

- surface modification: post-impact hardness
- ejecta: energy, angle, mass distribution
- etc

Anders (Univ. Kaiserslautern):

- amorphous Ar target
- Lennard-Jones potential
- 19 000 - 1 280 000 atoms
- up to 100 ps simulation time
- Ar_n cluster size n = 1 ... 10 000
- cluster energy E = 1 eV ... 50 keV

movie

Bringa (LLNL):

- Cu_n -> Cu
- cluster size n = 50 – 250 000
- target size: 0.25 – 25 x 10^6
- cluster energy: 10 eV / atom
- 0.5 keV – 2.6 MeV
- cluster velocity: 5.3 km / sec

Molecular dynamics simulations:
how to measure crater shape and volume

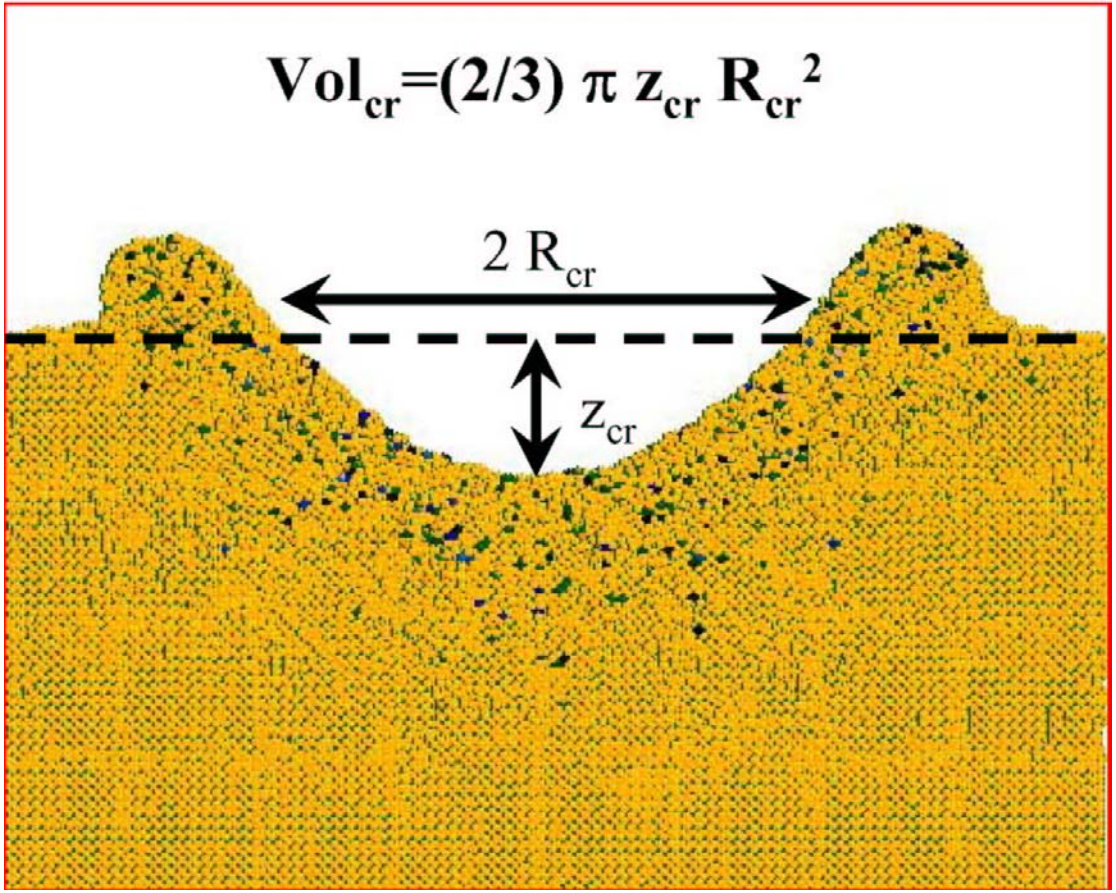

circular damage area

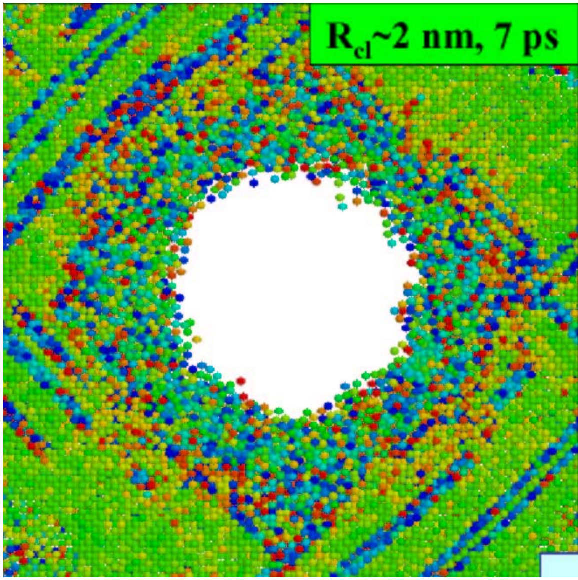

II.A. Cratering: systematic results for Ar system

Notation:

- V   crater volume (below reference plane), expressed as number of missing atoms
- z   crater depth
- r   crater radius
- r/z   aspect ratio

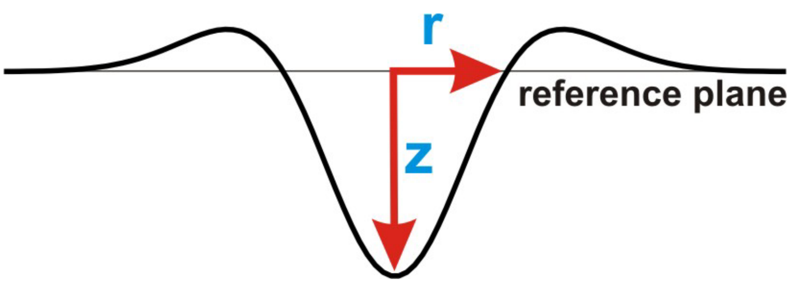

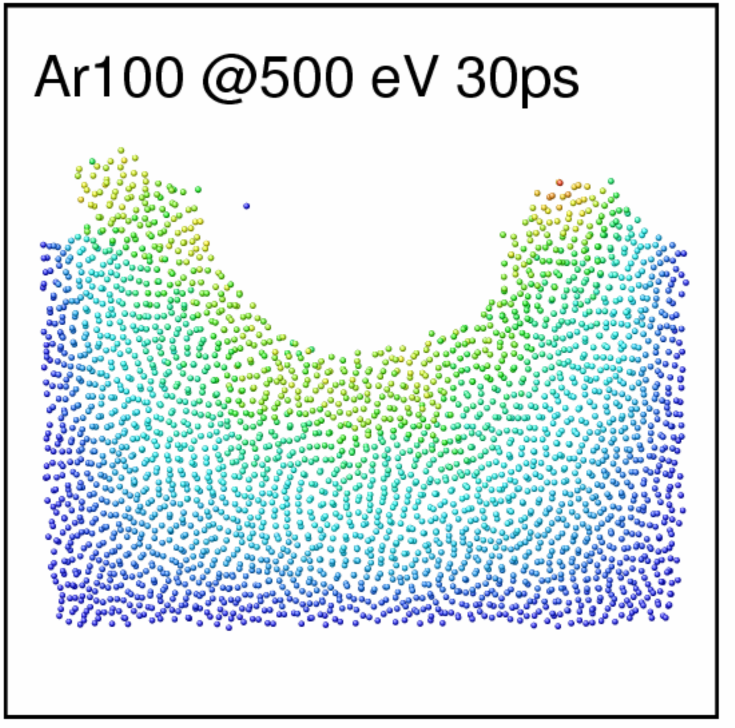

crater volume linear in energy

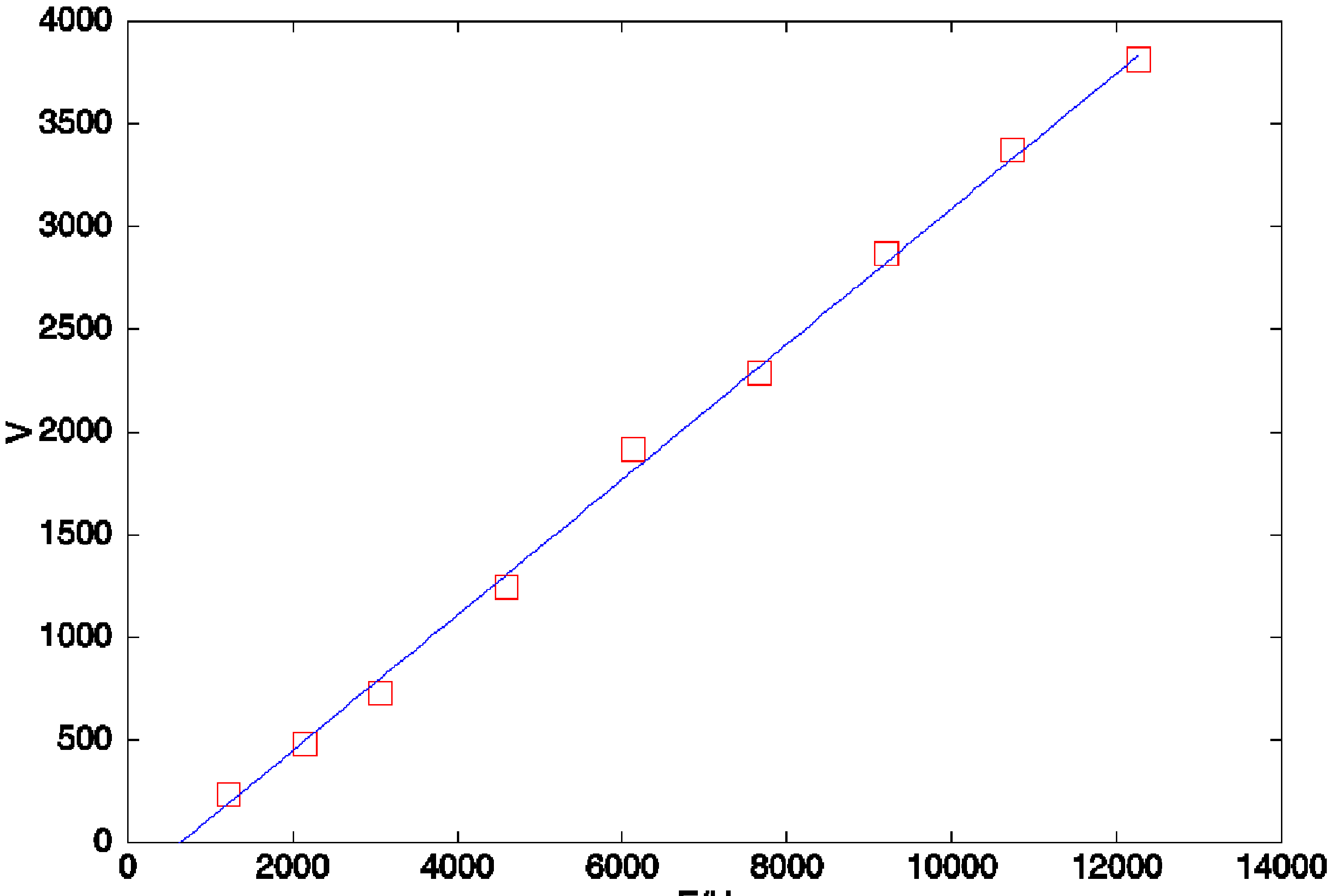

Ar_{100}

threshold energy to linear behavior

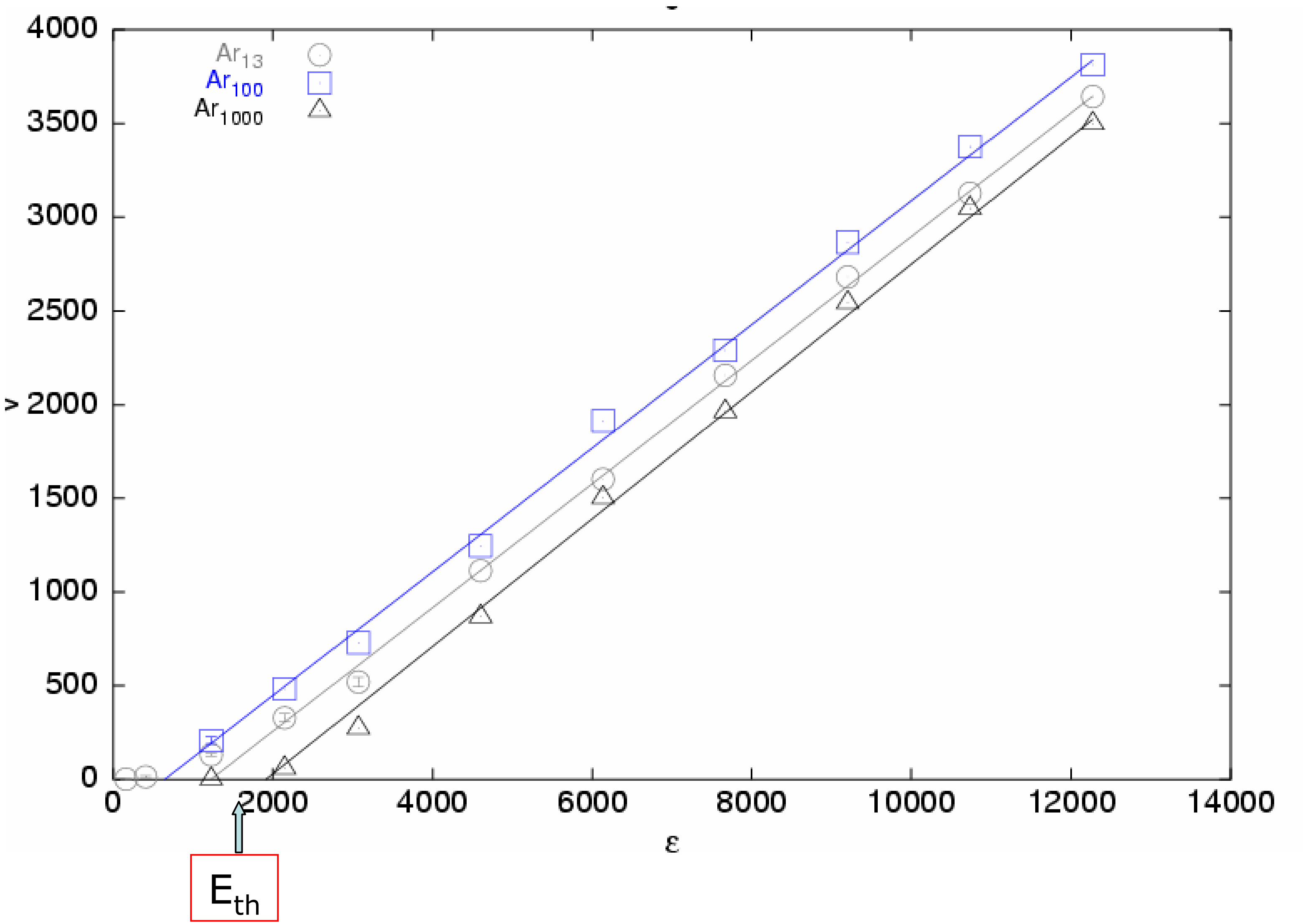

aspect ratio: nearly hemispherical craters

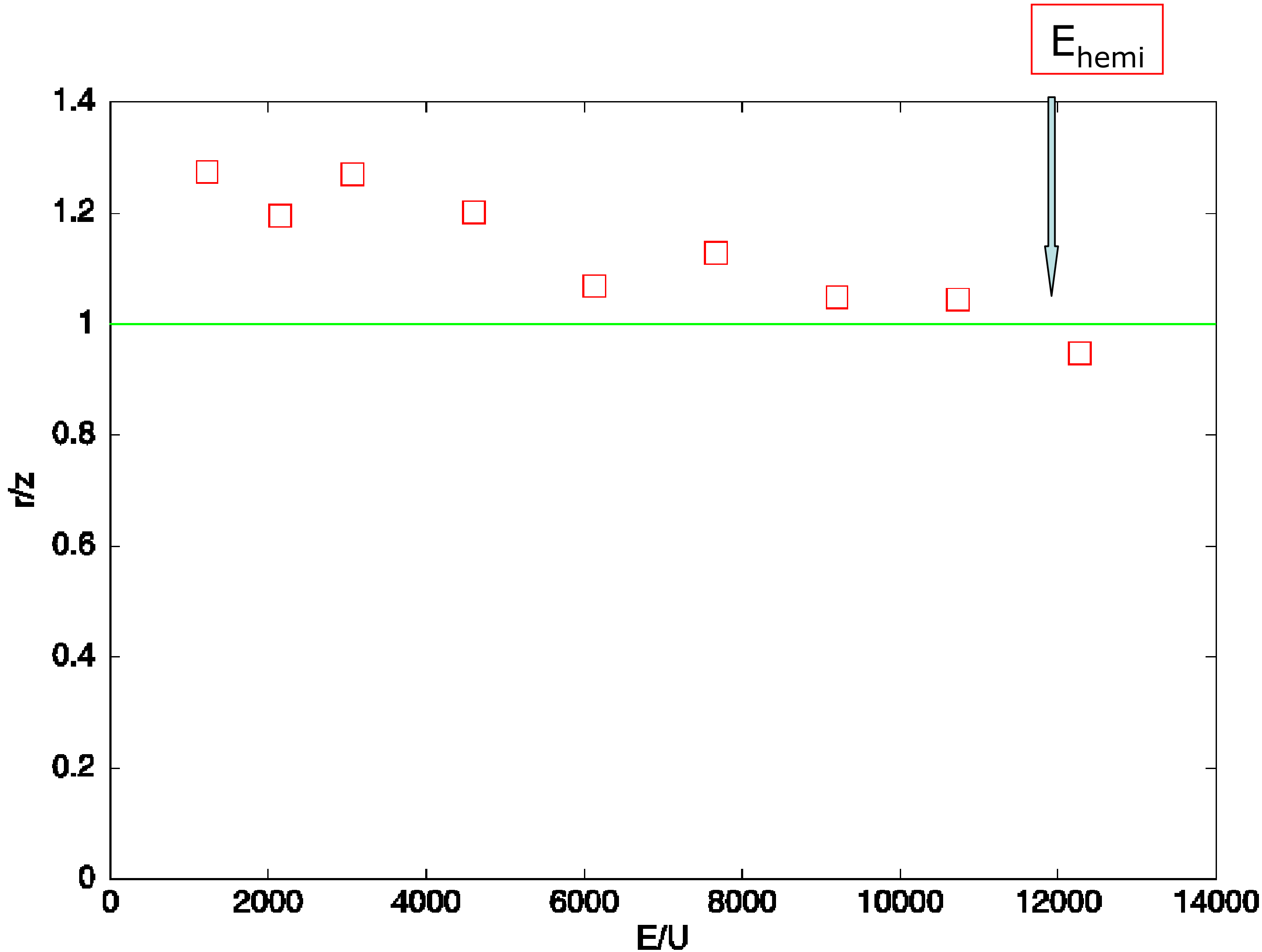

Ar_{100}

threshold energy to hemispherical crater

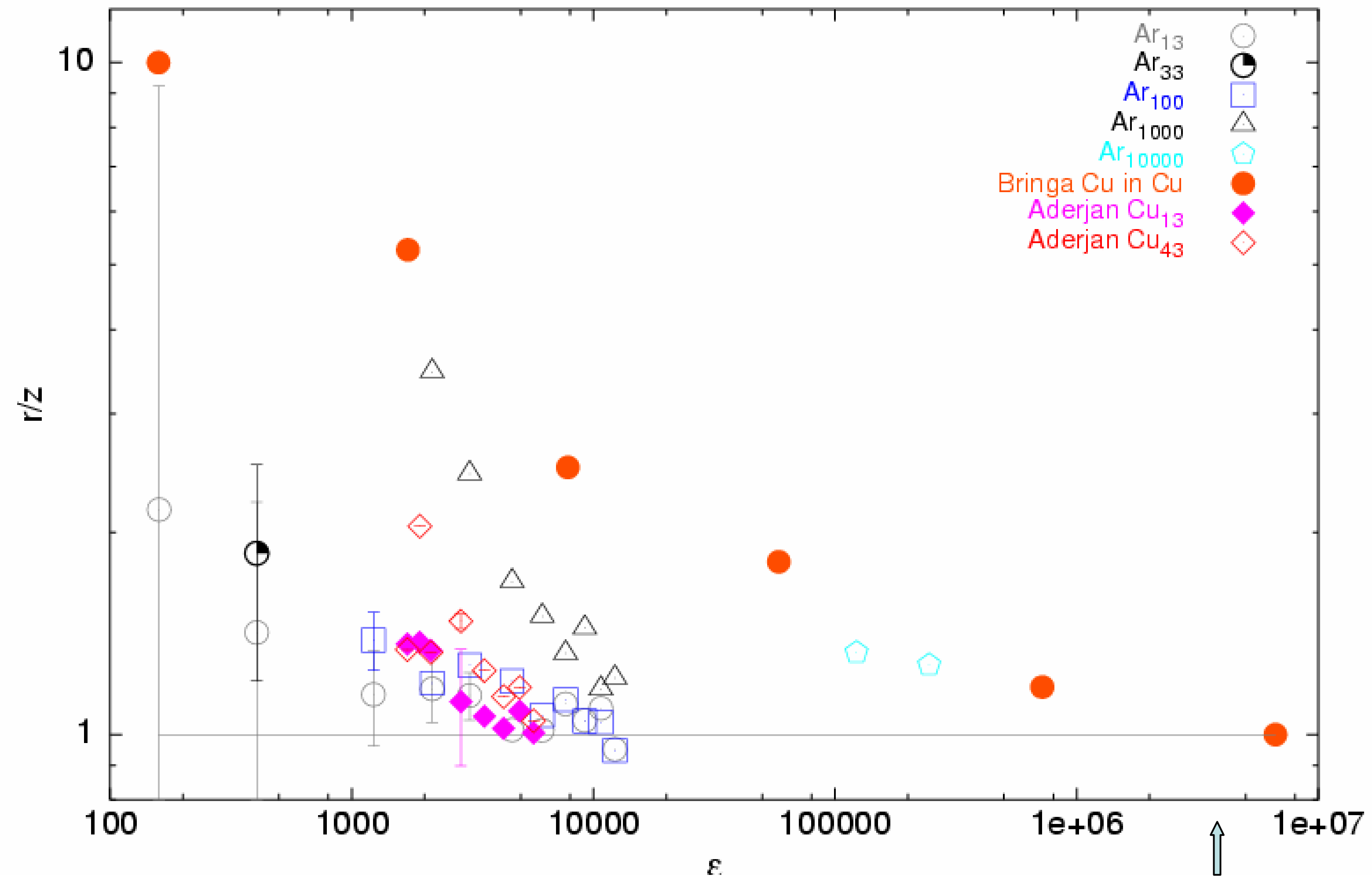

E_{hemi}

dependence of thresholds on cluster size n

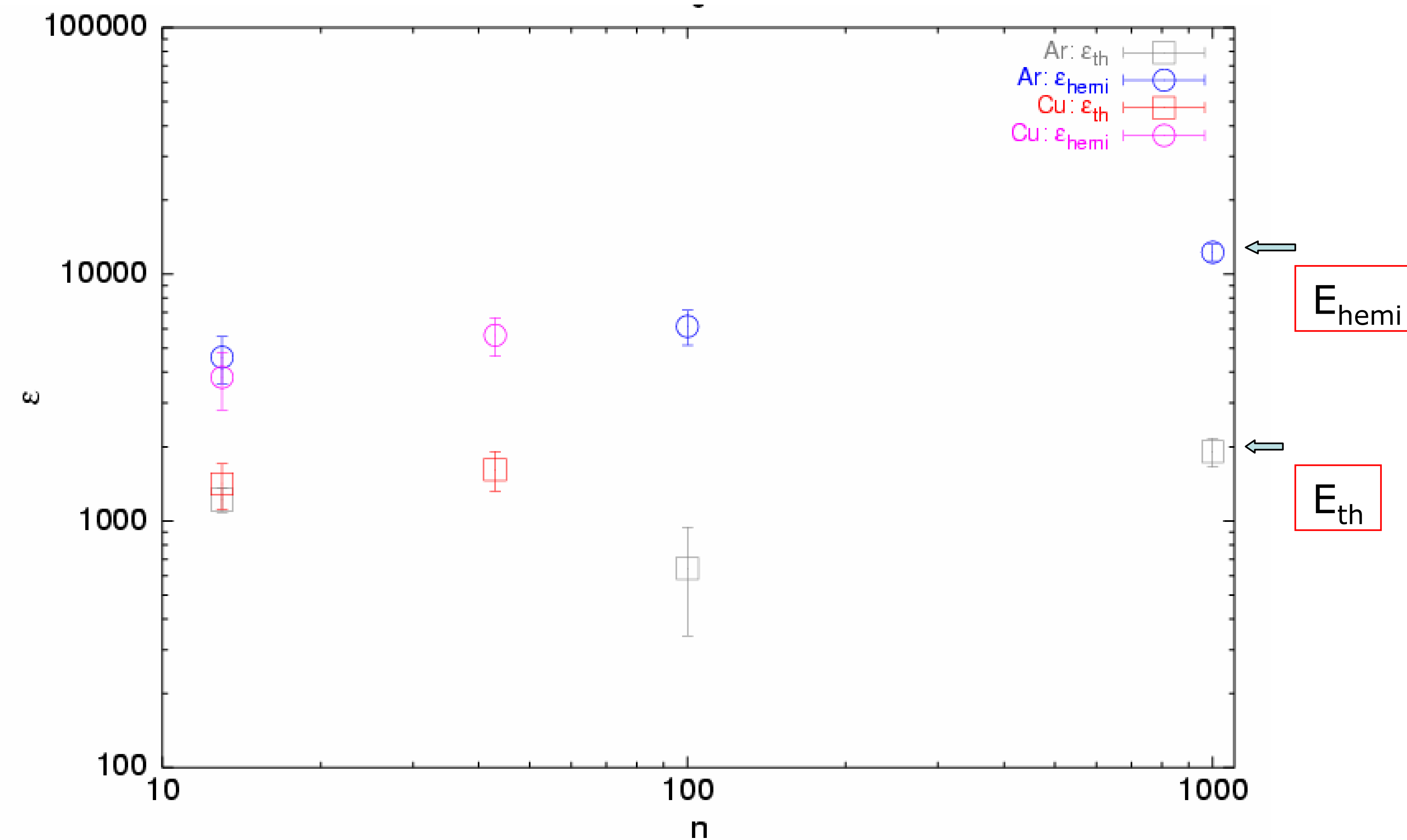

Cratering: pictorial results for Cu system

Crater formation mechanism:

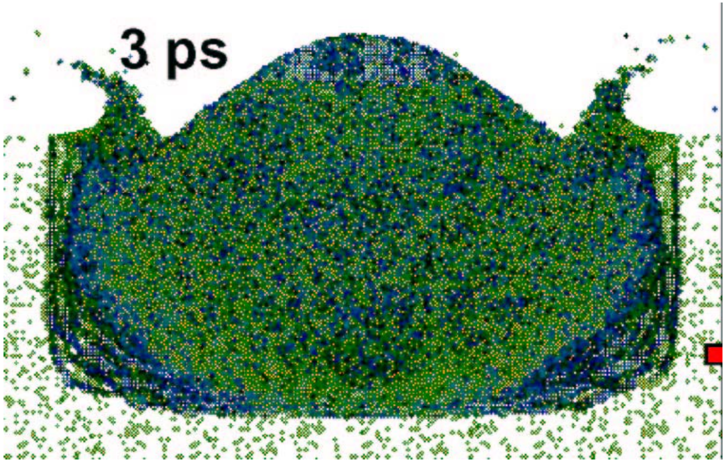

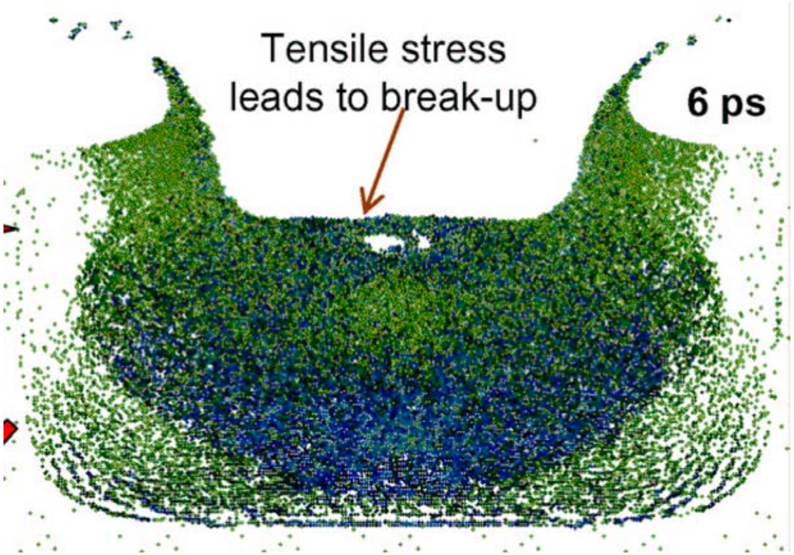

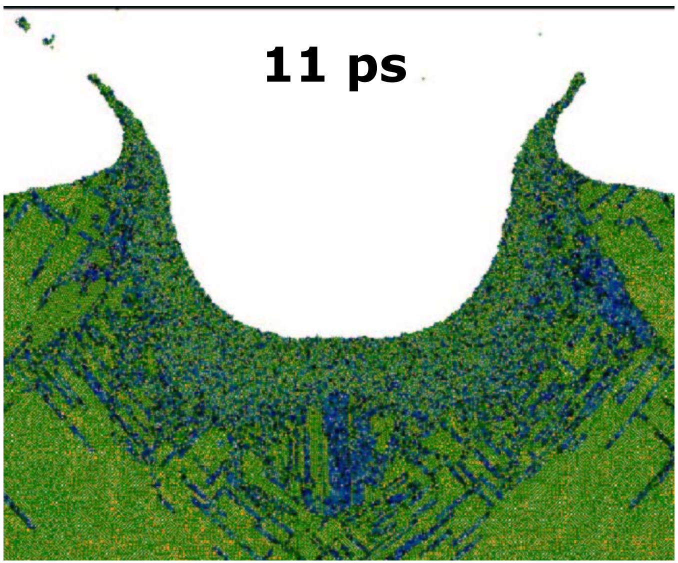

movie

R_{cl} = 9 nm
n = 250 000
E = 2.5 MeV

(stress coloring)

splashing:

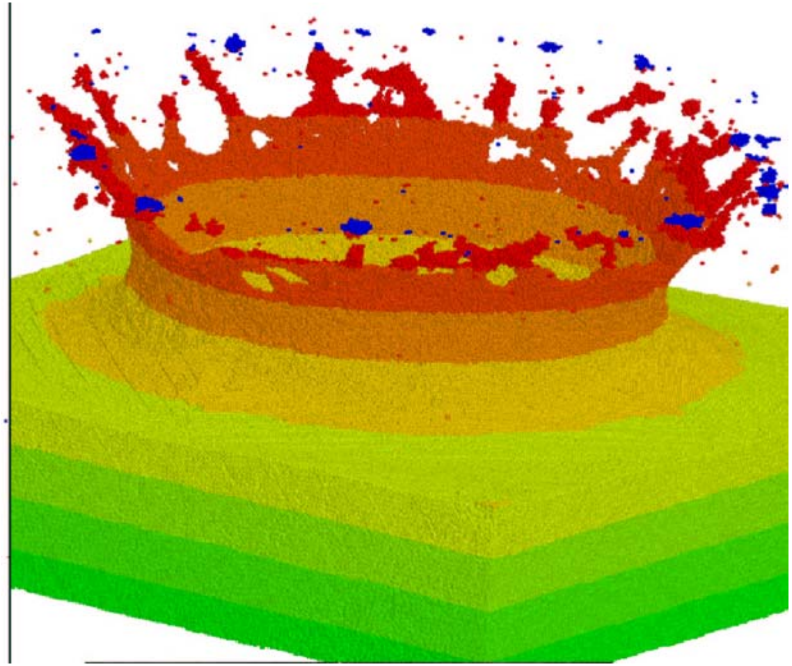

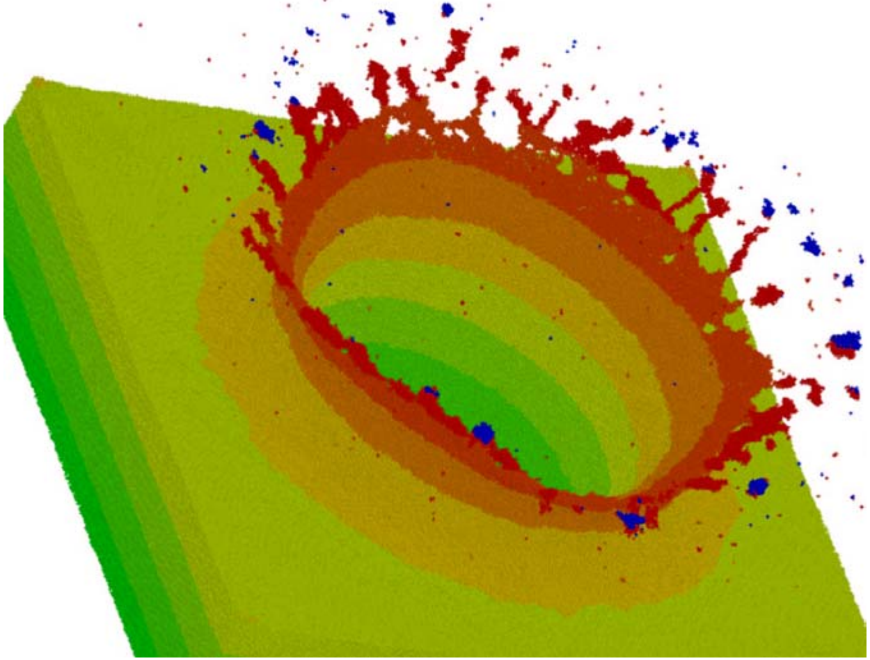

III Comparison to experiment

- Previous experiments on crater volumes:

- Rudolph 1969:
- µm-sized projectiles
- Eichhorn and Grün, 1993:
- ice targets
- Quinones and Murr, 1998; Murr et al 1998:
- mm-sized projectiles

- Previous simulations on crater volumes:

- Bringa et al, 2001
- Colla et al, 2000
- Aderjan et al, 2000

Crater volumes:
Synopsis (selection) of experiments and simulations

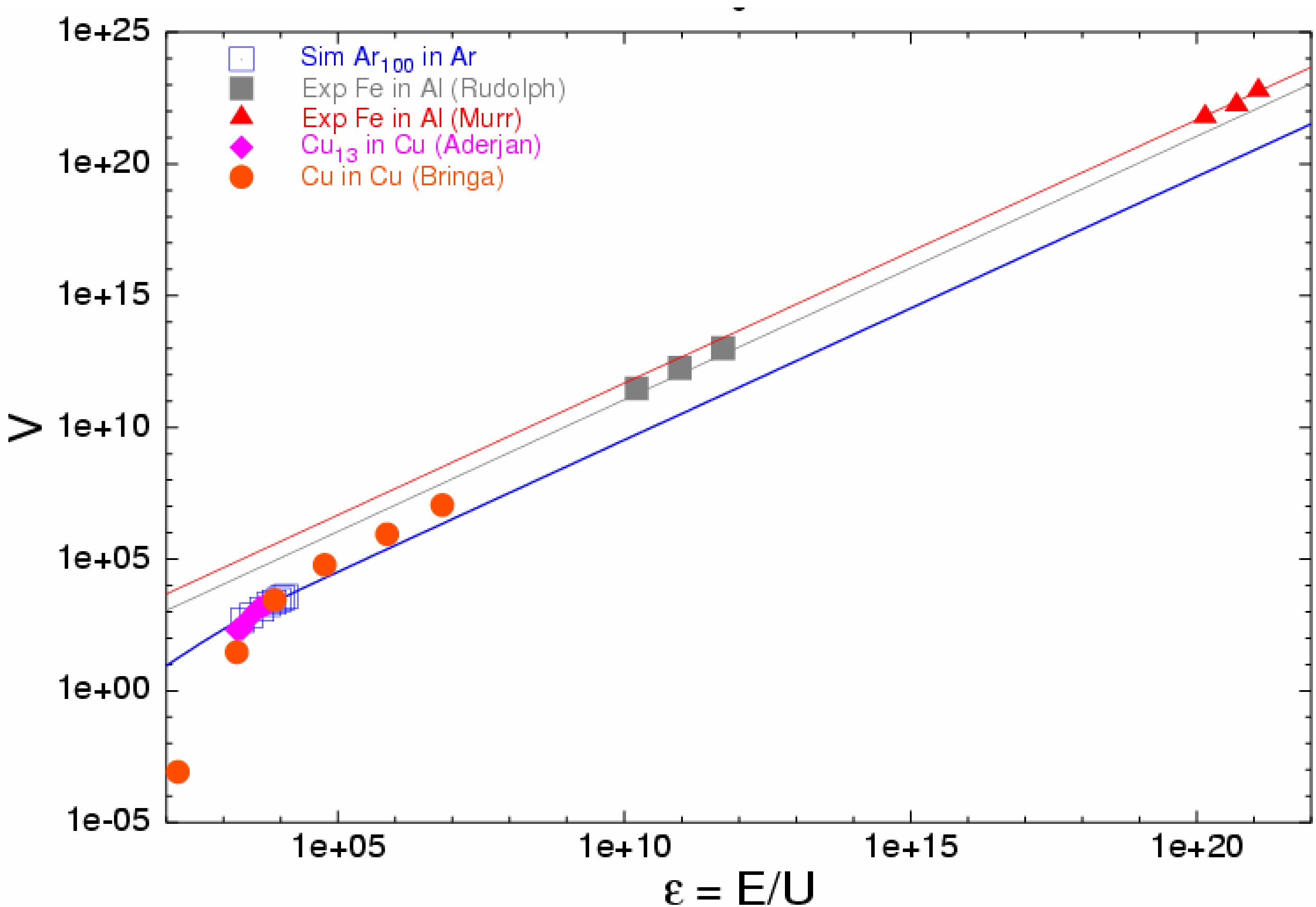

data scaled to cluster size n

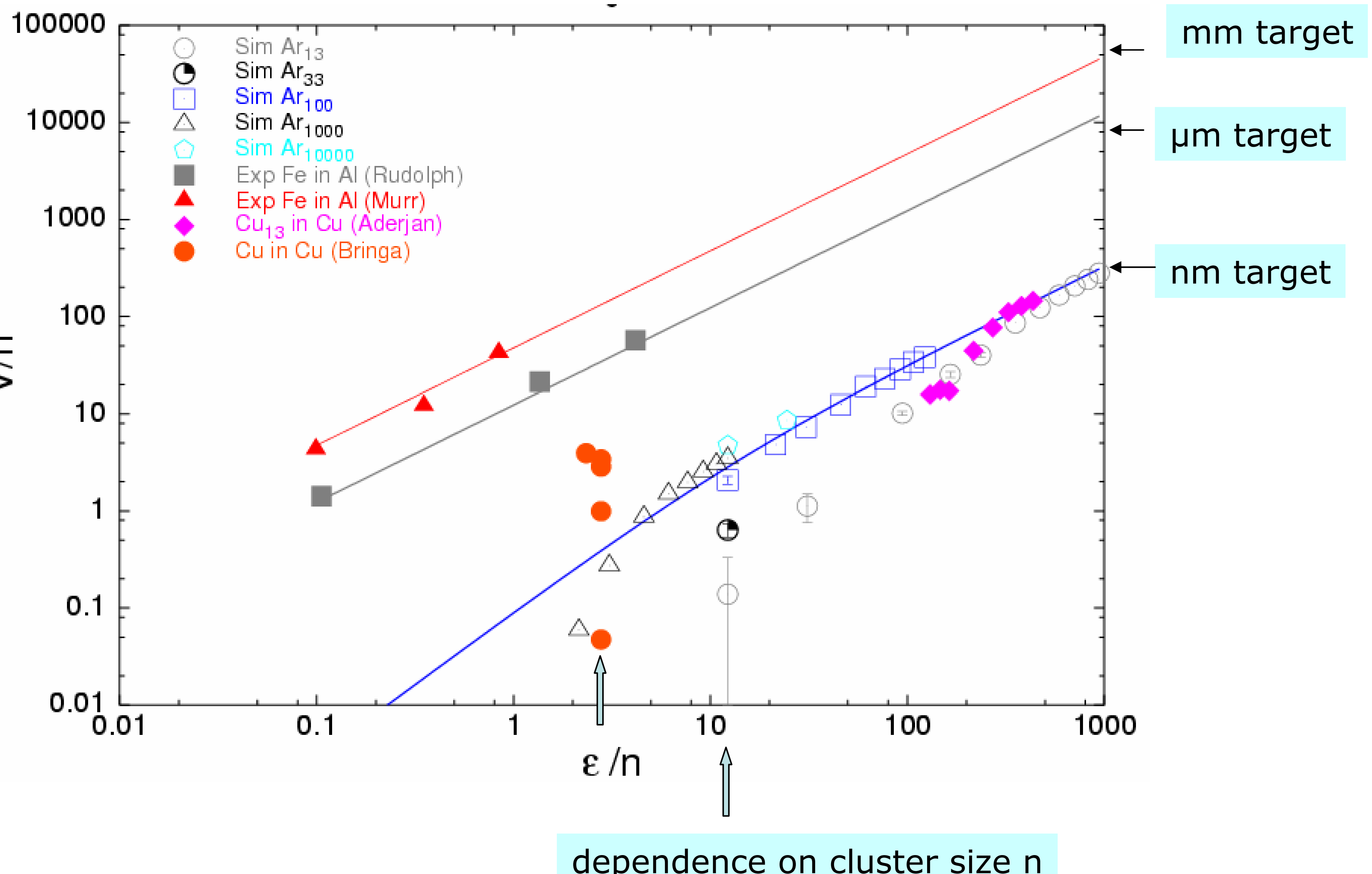

Conclusions

crater volume V

- linear in total energy E
- threshold energy to linearity ≅ hemispherical shape

  only minor dependence on cluster size
- results are „approximately" independent of projectile size and only scale with total cluster energy
- BUT: experiment for µm- and mm-sized projectiles give larger craters than simulations for nm-sized projectiles
- simulations for larger clusters show similar behavior
- probable reason: different dynamics for larger clusters

  - instead of „microexplosion" for small projectiles

  - stress effects (rebound pressure) within projectile important